UCRL 8926

UNIVERSITY OF CALIFORNIA

Ernest O. Lawrence

Radiation Laboratory

CHARGED–PARTICLE–INDUCED FISSION: A MASS SPECTROMETRIC YIELD STUDY

DISCLAIMER

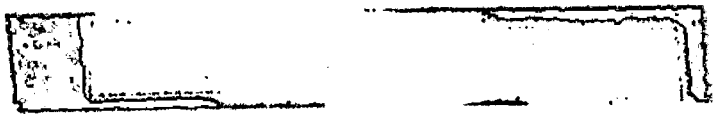

UCRL-8926

UNIVERSITY OF CALIFORNIA

Lawrence Radiation Laboratory
Berkeley, California

Contract No. W-7405-eng-48

CHARGED-PARTICLE-INDUCED FISSION: A MASS SPECTROMETRIC YIELD STUDY

Yung Yee Chu

(Thesis)

November, 1959

Printed for the U. S. Atomic Energy Commission

Printed in USA. Price $2.00. Available from the
Office of Technical Services
U. S. Department of Commerce
Washington 25, D.C.

CHARGED-PARTICLE-INDUCED FISSION: A MASS SPECTROMETRIC YIELD STUDY

Contents

Contents (cont'd.)

CHARGED-PARTICLE-INDUCED FISSION: A MASS SPECTROMETRIC YIELD STUDY

Yung Yee Chu

Lawrence Radiation Laboratory and Department of Chemistry
University of California, Berkeley, California

November, 1959

ABSTRACT

The products from the fission of uranium induced by charged particles were studied in a mass spectrometer. Both U^{238} and U^{235} were bombarded with 45.7- and 24-Mev helium ions, and U^{238} was also bombarded with 730-Mev protons and 100-Mev carbon ions. The total chain yields in the region of the rare earth elements (mass 140 to mass 155) for most of the above bombardments and a thermal-neutron bombardment of U^{235} were studied by using the isotopic-dilution technique. Independent yields were measured for all the above bombardments for several shielded nuclides.

The total chain yields in the mass region 140 to 155 constitute a smooth portion of the yield-mass curve, showing no obvious perturbations. The fractional-chain-yield results show that the charge distribution agrees best with the equal-charge-displacement rule, provided linear Z_A values are used. In other words, the obvious shell effect in the Z_A used in the fitting of thermal-neutron data is not appropriate in the medium-energy fission (24- and 45.7-Mev helium ions here). The indications are that this process is closer to the higher-energy fission mechanism. A more practical distinction between the low-energy fission and the high-energy fission would be required. It seems that the mechanism for the medium-energy fission should be somewhere between the equal-charge-displacement rule using "non-shell-affected Z_A" and the constant charge-to-mass ratio rule.

The broad and asymmetric-shaped independent yield distribution for higher-energy fission (730-Mev protons) with a given element was observed.

This can be explained by the multiplicity of fissioning nuclei. In 100-Mev carbon-ion fission of U^{238}, the distribution showed a similar effect, but not as striking.

The contribution of fission induced by secondary-neutrons in all the cyclotron bombardments was discussed. From the results of some other studies and the indications of this work, the contribution cannot be significant.

The composition of stable isotopes of Ce, Nd, and Sm formed in high-energy fission is discussed. It has been concluded that it is not impossible that the natural abundance of these elements may be, in part, due to some kind of high-energy fission of heavy elements.

INTRODUCTION

The mass spectrometer has been used for years as a precise instrument for isotopic analysis, and the isotopic-dilution technique[1] is one of the most sensitive methods for quantitative determination. The combination of the two constitutes a valuable means of determining isotopic compositions of small samples ($\ll 10^{-6}$ g), such as may be produced in nuclear reactions.

The main purpose of this work is to take advantage of the precision of this method in the measurement of yields in fission induced by charged-particle irradiation. We have bombarded natural uranium with 24- and 45.7-Mev helium ions, and highly enriched U^{235} with 45.7-Mev helium ions, also natural uranium with 730-Mev protons; in addition, U^{235} was irradiated with thermal neutrons. Total chain yields were measured for those products in the rare earth region. Independent yields of several shielded nuclides (from mass 83 through mass 154, including isotopes of Rb, Cs, Pm, and Eu) were measured for the above bombardments plus bombardment of U^{235} with 24-Mev helium ions and of a target of natural uranium with carbon ions of average energy 100 Mev in the Hilac (Heavy-ion Linear accelerator).

Thode[2] and Thode and Graham[3] were among the first to use the mass spectrometer to investigate the isotopes of Kr and Xe resulting from the fission of U^{235} by thermal neutrons. Later, this technique was extended to other fission products from thermal-neutron-induced fission of U^{235},[4-10] and of U^{233},[9,10-12] and to fast-neutron-induced fission of U^{238}.[8] However, all these investigations gave only relative yields between isotopes of a given element. Not until Petruska et al.[13,14] used the isotopic dilution method along with the mass spectrometer were 28 absolute fission yields of U^{235} measured (mostly of heavy fragments). About the same time, Glendenin et al. did similar work.[15] Then Blades, Fleming, and Thode used this method to determine the ratio of Xe to Kr in U^{235} fission.[16] Kukavadze et al., in Russia, later measured the thermal neutron fission yields of U^{233} in the mass region 140 to 150 with the same technique.[17] Recently more results of this same

experiment have appeared.[18] Gorshkov et al. have measured the yields of U^{235} fission products in the rare earth region by means of an integral mass spectrometer method.[19]

From the above brief summary, it is obvious that this technique had been used mostly for thermal-neutron-induced fission, while the rest of the domain of nuclear fission remained uninvestigated by this approach. On the other hand, fission induced by charged particles had been studied considerably by radiochemical techniques. For a few examples: Ritsema,[20] Wade et al.,[21] Vandenbosch et al.,[22] and Thomas[23] studied fission induced by helium ions with energies between 18 and 48 Mev on various uranium isotopes; Gibson[24] and Lessler[25] investigated fission of various isotopes of uranium by deuterons of energy less than 24 Mev; many workers studied fission induced by relatively high-energy protons, deuterons, and helium ions ($>$ 50 Mev).[26-37] Among recent works of this type, Stevenson et al. studied fission induced by protons (10 to 340 Mev) and deuterons (20 to 190 Mev),[38] and Pavlotskala and Lavrukhina measured fission yields from uranium fission induced by 660-Mev protons.[39]

For several experimental reasons, we picked the rare earth region as the area of interest for total-chain-yield studies. The most important of these reasons is that this choice gives the largest single continuous mass region that can be studied by the mass spectrometer at high sensitivity. In addition, the comparative rarity of the lanthanides should reduce the natural contamination problem referred to below.

As Inghram pointed out,[1] the main limitation of the stable-isotope-dilution method is the natural contamination, rather than chemical recovery or the sensitivity of the mass spectrometer. This was no problem in the thermal-neutron fission of U^{235} and U^{233}, since large neutron fluxes and long periods of irradiation were possible, and both U^{235} and U^{233} have fairly large thermal-neutron fission cross sections. But for fission induced by charged particles, both the beam intensity and the cross section are relatively low, and the bombardment time is necessarily much shorter. For most of the targets we have studied, the amount of the most prominent isotope produced is about one millimicrogram or less. At this millimicrogram level and below, the

natural "rare" earth elements are quite "abundant" from all sources, such as the target material, reagents, even dust particles. The main effort in the first half of this work was to purify the target material and all the reagents used, and to take every precaution to lower the natural contamination. This is discussed in more detail in the next section.

Since low-energy fission usually gives primary fission products with large neutron excess, the independent yields of most of the shielded nuclides near stability are rather low. In most cases, the observation of shielded isotopes served as a measure of the natural contamination. Thus this contamination could be subtracted out rather accurately. This kind of subtraction has been used quite often in this work and is discussed again in the section on calculation.

A U^{235} target was irradiated in the thermal column of the LPTR (Livermore pool-type reactor) at the Livermore Radiation Laboratory. In this repetition of previous work[14,15] there was a slight modification--that is, a much shorter irradiation time (3 days compared to several months[14]) was used, with a neutron flux of 6×10^{11} neutrons/cm^2/sec. Consequently, a much smaller neutron-capture correction was necessary.

The other phase of this work is the measurement of the independent yields of shielded isotopes, which leads to the interesting problem of charge distribution in the fission process. (This is the distribution of the primary yields along an isobaric chain.) The two most commonly used empirical rules for correlation of experimental results are the Equal-Charge-Displacement (ECD) and the Constant-Charge-to-Mass-Ratio (CCR) rules.

The former rule was first proposed by Glendenin, Coryell, and Edwards,[40] and later modified by Pappas.[41,42] This rule proposes that the effective β-decay chains for a fragment pair are of the same lengths, that is,

$$(Z_P - Z_A)_H = (Z_P - Z_A)_L ,$$

where Z_P is the most probable charge of the primary product for a given

mass A, Z_A is the most stable charge for mass A; the subscript H stands for a heavy fragment and L for its complementary light fragment. Glendenin et al. used this rule for the observed products[40] and they used a continuous Z_A function. Pappas proposed the consideration of primary fission fragments before neutron boil-off, and he used a Z_A function which included the discontinuities in the stability valley at shell closures.[41] The rule has been proved most appropriate for low-energy fission, especially for thermal-neutron fission.[43,44]

The constant-charge-to-mass-ratio rule was first set forth by Goeckerman and Perlman.[45] They proposed that a most probable charge was found for a ratio of charge to mass equal to that of the fissioning nucleus. This rule has been used more often for high-energy fission.[29,30] Gibson has studied the charge distribution for medium-energy reactions (20.6- and 23.4-Mev deuterons on Pu^{239} and U^{233} respectively, and 31.5- and 45.7-Mev helium ions on Np^{237}).[24] He found that the charge distribution was more consistent with the CCR rule; but from the shape of the distribution and the integrated area under the curve, he concluded that the actual charge distribution may be intermediate between the two rules considered. In a slightly lower energy region, Alexander and Coryell found results[46] which were more consistent with the ECD rule. Recently del Marmol has studied U^{235} fission induced by 13.6-Mev deuterons and 23.5-Mev helium-ions,[47] and also found results which were consistent with the ECD rule.

It was with this background in mind that we undertook the study of charge distribution, hoping that more precise experimental data added to the existing picture might clarify some of the doubts and bring about a better understanding of nuclear charge distribution.

EXPERIMENTAL PROCEDURES

The Target

Target Materials

Purified U_3O_8 of natural uranium and enriched U^{235} (with the composition of 93.2% U^{235} and 6.8% U^{238}) were used as target materials. Since the limitation of the isotopic-dilution technique is mainly due to natural contamination of the elements studied, the essential effort in this work was to eliminate this interference.

The purification procedure was as follows: Chemically pure uranium foil was dissolved in concentrated HCl and a few drops of concentrated HNO_3. After the foil had completely dissolved and the small amount of HNO_3 was expelled, the solution was allowed to cool and then was run through an anion-exchange column (Dowex-1) in a dust-free box. All the rare earths were eluted with conc. HCl solution while uranium remained on the column. The column was washed with conc. HCl for several column volumes and then the uranium was taken off with dilute HCl (~1 M). The eluant was made up to conc. HCl with HCl gas and run through another clean anion-exchange column (the column had been washed with a large amount of conductivity water and HCl of various concentrations). The purification process was repeated three times. The purified uranium solution was then made alkaline by adding conc. NH_4OH, and uranium was precipitated as hydroxide. Then it was centrifuged and heated in a platinum crucible at about 1000°C until converted to U_3O_8 powder.

Target Preparation

Since the final form of the purified uranium is powder, and electrodeposition is not applicable for the thickness and the amount of target material required, the target was made by pressing the U_3O_8 powder into a trough on a copper piece which was made to fit the accelerator target holder. The shape and the depth of the trough were made to match the collimator used and to give the desired energy loss in the target. The depth of the trough for the 60-inch cyclotron bombardments ranged from 2.5 mils (0.0025 inch) to 3.5 mils, depending on

the bombarding energy. The pressing was carried out by means of a hydraulic press. An ordinary microtarget[20,25] was used for the 60-inch cyclotron bombardments, and a "clothes-pin" target holder for the 184-inch cyclotron bombardments. In most of the cases, 1-mil aluminum foil was used as the front guard foil; sometimes 0.5-mil platinum foil was used. For low-energy bombardments, other front foils were used to give the desired energy degradation. All the degradations of energy were carefully calculated from the range-energy curves of Aron, Hoffman, and Williams[48] and the range-energy curve for carbon ion.[49] The neutron target was made by sealing the $U^{235}_3O_8$ powder in a quartz capsule tube, then it was put into an aluminum can for the thermal-neutron irradiation.

Target Bombardments

Most of the targets were bombarded intermittently over an extended period of time ("Stand-by Target"), and the accumulated current was summed up from individual runs. The total beam current for each bombardment was recorded for use in making decay corrections. All long-stand-by targets were allowed to cool over a period of several months to allow all the rather short-lived isotopes to decay, thus enabling us to study total chain yields. For the independent yield studies, short bombardments (about 2 to 3 hours) were made and the samples were run shortly after the bombardment. For the 60-inch cyclotron bombardments, the average beam intensity was about 15 to 20 microamperes, and the total beam current of several bombardments made over periods of 2 weeks to 1 month were 200 to 350 μah for a typical long-stand-by target. The long-bombarded 184-inch cyclotron target had 25 μah in 25 hours' bombardment time within 1.5 months. Several short bombardments with C^{12} were made for independent yield measurements of cesium isotopes with total beam of about 1 to 2 μah for a few hours' bombardment.

Chemistry

General Procedure

As mentioned in the Introduction, the greatest experimental restriction on the sensitivity of this measurement is natural contamination

rather than the sensitivity of the mass spectrometer. Therefore the procedure was made as free of natural isotopes as possible. After a long period of careful individual step checks, it was found that every step in our ordinary chemistry contributed some of the total contamination. Thus all the reagents were purified, and the whole procedure was made of such simplicity that all steps not of absolute necessity were eliminated. The procedure used was as follows: First the target of U_3O_8 was dissolved in conc. HCl and a few drops of conc. HNO_3. After the dissolution, the trace of HNO_3 was expelled. The solution was allowed to cool and was divided into two exactly equal samples. To one sample was added an accurately known amount of certain separated stable isotopes of the elements to be measured. The solutions were adjusted to about 4 M HCl, then passed through two separate but identical anion-exchange columns (Dowex-1) in order to eliminate the mass of the target. The eluants* were then evaporated almost to dryness, and made to 1 M HCl in a very small volume (few drops). Each was equilibrated with a small batch of clean cation-exchange resin (Dowex-50, which had been washed exhaustively on the column with high-pH eluting solution to wash off all the natural rare earth elements), until most of the activity was absorbed by the resin. Then the resin batches were loaded on two identical cation-exchange columns for individual rare-earth separation.[50] The eluting solution used was 1 M ammonium lactate with pH ranging from 3.10 to 3.45. After the individual rare earths were separated (only from Eu to Ce), the individual fractions were made alkaline by adding conc. NH_4OH and then passed through rather small anion columns separately. The columns were packed with Dowex-1, and had a layer of ferric hydroxide precipitated on the top 1/4 in. of the resin bed. The ferric hydroxide layer was put on the column by first absorbing a few drops of ferric chloride from conc. HCl, and then converting to hydroxide by passing ammonium hydroxide through the column. Thus each individual rare earth element was retained

*Actually many of the fission products were eluted from this column. A step for separation of the rare earths, either by adding carrier or by solvent extraction, gave too much contamination. Only this simple procedure was used, and was proved applicable by further experience.

by the ferric hydroxide layer and the lactate solution passed through. The column was washed with a small volume of dilute NH_4OH and then the rare earths were taken off in a few drops of conc. HCl, collected on clean platinum discs, and dried under an infrared lamp. The chlorides were changed to oxides by adding 1 to 2 drops of conc. HNO_3 and were then ready for the mass spectrometer runs.

Reagents

Special precautions were taken with the reagents used throughout the whole process. The conc. HCl was made by bubbling gas from an HCl tank through several wash bottles and traps, and finally dissolved in conductivity water in a quartz vessel. The conductivity water was obtained by running distilled water through two large ion-exchange columns, one anion and the other cation. The nitric acid was purified either by successive TBP (tributyl phosphate) extractions or by re-distillation, then collected in quartz vessels. The conc. NH_4OH was made by passing ammonia gas from the tank through several wash bottles and traps into conductivity water in a clean polyethylene bottle. The lactate solution was purified by passing conc. lactic acid (~5 M) through a large cation-exchange Dowex-50 column at low pH, (rare earths remained on the column). Thus the lactate was purified several times. The purified lactate can be made to desired concentration and adjusted to the correct pH by adding NH_4OH.

Column Chemistry

Ion-exchange resins were used very much in this work, starting from the purification of the target material, throughout the chemical procedure, and through the final preparation of the sample for the mass spectrometer run. They were chosen not only because of their neatness and simplicity in operation, but also because of their desirable eluting properties for various purposes in this work. As mentioned before, the sorption behavior of the rare earth elements with the anion-exchange resin[51] gave satisfactory purification of the target material, and later, the separation of the gross fission products from the target. But the separation of the individual rare earths by means of cation-exchange resin

(Dowex-50) was the most important, because there is no other equally convenient way of separation. The column used for this purpose was about 5 to 6 mm in diameter and the resin bed was about 15 cm long. The column was heated by using trichloroethylene vapor (about 87°C). Usually a small amount of freshly bombarded U_3O_8 was added to the cooled targets in order to identify the various rare earth elution peaks by the activity. (The amount of freshly bombarded target was very small so that it would not affect appreciably the atomic composition of the cooled target). A typical elution curve is shown in Fig. 1. It will be noted that the "valleys" are not free of activity, but it must be remembered that many fission products other than rare earths are present.

For the majority of the independent yield measurements, short bombardments were used and no cation-column separation was required. Cesium has the highest ionization efficiency in the mass spectrometer, and it evaporates from the sample filament at lower temperature than most other elements, hence no separation from other fission products was necessary. Similar separations in the mass spectrometer could be made for Rb.

Spiking Solutions*

The spiking solutions were made by weighing a known amount of separated isotope of the particular element of interest. For example, stock solutions of Ce^{142}, Nd^{144}, Sm^{144}, and Eu^{151} were made and diluted by known amounts in order to get the desired concentrations ($\sim 10^{-12}$ g/μl). Ce^{142} was chosen because it is the minor constituent in natural isotopes, Nd^{144} is partially blocked by Ce^{144}, and the other two are shielded nuclides. Therefore they served as good spiking samples. The concentrations of the dilute solutions were chosen so that a reasonable amount (e.g., 25 to 500 μl) of the dilute spiking solutions gave amounts

*The word "spike" is used in this work to represent the addition of the enriched isotopes to the sample, in analogy to the word "spike" as defined in Webster's Unabridged Dictionary: "To add alcohol or strong spirituous liquor to beer or nonalcoholic beverage (slang, U.S.)".

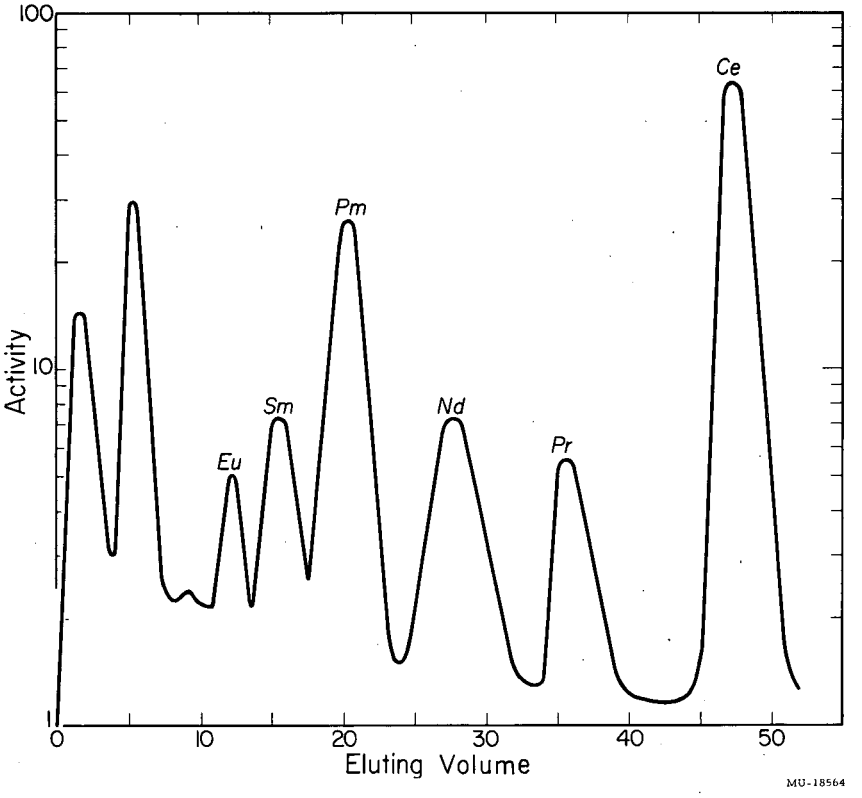

Fig. 1. Elution curve of the light rare earth elements. (coordinates in arbitrary units).

of the added elements comparable to the amount of the adjacent isotopes made in the reaction (estimated from radiochemical yield mass curves). These spiking solutions have been cross-checked in the mass spectrometer with solutions of natural composition for their concentrations and compositions.

The Mass Spectrometer

The spectrometer used was a single-directional focusing mass spectrometer with a 60-degree sector and 12-inch radius of curvature. The positive ion beam is generated thermally by evaporation of the metal oxide from a tungsten filament to a hot rhenium filament. Then ions emitted from the rhenium filament were collimated by the collimating plates of the source and directed normally into a wedge-shaped magnetic field which resolved the ion beam into its various mass components. The mass-separated positive ions were detected by means of an electron-multiplier and integrated by a vibrating-reed electrometer,[52] and the output was recorded on a Leeds and Northrup recording potentiometer. This machine, in general, is quite similar to the one described by Nier.[53]

The machine incorporates a Stevens-type vacuum lock,[54] and one can change samples without letting down the machine to air, thus reducing the time required to begin the mass analysis. The operating pressure of the system is about 1×10^{-8} to 2×10^{-8} mm Hg as measured by a modified Bayard-Alpert type of ionization gage. A proton resonance fluxmeter was used to establish the mass scale. The measurements were taken by an automatic, continuous sweep of the analyzer magnetic field over the desired mass region. The spectra were repeatedly scanned until good statistics were obtained.

TREATMENT OF DATA

Chain Yields

Unspiked Sample

Measurement of the unspiked sample established the relative yields among the isotopes of an element made in a certain reaction. After the raw data had been tabulated, all the contributions from other elements had to be subtracted. For example, in the Nd fraction, if there was a peak corresponding to Ce^{140} (though mass 140 does not contribute directly to the Nd spectrum), a correction was required for the corresponding contribution of natural Ce^{142} to the Nd spectrum. The individual rare-earth separation precluded a significant contribution from other elements made in the reaction, therefore this kind of correction can be made very easily. However, there were cases of ambiguity (which are discussed later). Sometimes there were more than one correction for other elements. For instance, in the Sm fraction, corrections were sometimes necessary for both Nd (on mass 144, mass 148, and mass 150) and Eu (on mass 151). Table I illustrates this effect.

A correction was also made for natural contamination of the element being considered. As mentioned before, this is the crux of the whole work. If the natural contamination level were much higher than the amount made in the reaction, the spectrum would be very similar to the natural composition and it would be impossible to determine the target composition accurately. On the other hand, even if the contamination level were comparable to or somewhat lower than the amount made in the reaction, and there were no accurate way to correct for this natural contamination, the data would still not be of much value. The greatest effort in this work has been concentrated on lowering the contamination level, and we have reached the point where the contamination level is lower than the amount made in the reaction for most of our bombardments. However, we still have to have an accurate means of subtracting the natural background. Fortunately this is of importance primarily at high excitation energies. In lower-energy fission, the primary fragments are on the neutron-excess side of stability, therefore the independent yields of most of the natural

Table I

Isotopic composition of Sm fraction from fission of U^{238} induced by 45.7-Mev helium ions (an example of the corrections for contamination)

Mass	Observed	Natural Nd	Natural Eu	Gross Sm	Natural Sm	Corrected Sm
144	0.0106	0.0026		0.0080	0.0080	
145	0.0009	0.0009				
146	0.0019	0.0019				
147	0.1288			0.1288	0.0382	0.0906
148	0.0292	0.0006		0.0286	0.0286	
149	1.0000			1.0000	0.0351	0.9649
150	0.0474	0.0006		0.0468	0.0190	0.0278
151	0.7448		0.0404	0.7044		0.7044
152	0.6425			0.6425	0.0676	0.5749
153	0.0442		0.0442			
154	0.4251			0.4251	0.0572	0.3679

isotopes which are shielded from the β chain are rather small. For those isotopes on the neutron-deficient side, the independent yields are virtually zero. This is still true in the main in the medium-energy fission (24- and 45.7-Mev helium ions in this work), as is discussed later in some detail. Because the observation of the amount of neutron-deficient isotopes determined the contamination level, therefore a residual peak after the contribution from all other elements had been subtracted (if there were any other elements present), was attributed to natural contamination. Thus all the other stable isotopes observed can be corrected with respect to this one by using the known natural composition.

An example is given in Table I to illustrate the above explanation. This is the Sm fraction from a U^{238} target bombarded with 45.7-Mev helium ions. The second column gives the direct observations, the third and fourth columns give the contributions from natural Nd and Eu respectively. The fifth column is the composition after correction for these two

elements. The chain position* for Sm^{148} is 3.64 (using our own method to calculate Z_p, which is discussed later), and the only β chain precursor, Pm^{148}, has chain position 2.64, both values of chain position predicting very low independent yields. ($\ll 1\%$ of the chain). Therefore all the Sm^{148} can be considered as natural Sm, and the other stable isotopes can be corrected for contamination by using the natural composition. The last column is the composition (in arbitrary units) of the Sm fraction made in the reaction. Sm^{147} is only a partial chain, since the 2.64 yr Pm^{147} has not fully decayed. Sm^{150} and Pm^{150} are shielded from the β chain by Nd^{150}, therefore the Sm^{150} yield represents the independent yield of Pm^{150} plus the much smaller yield of Sm^{150}. Of course one can also use Sm^{144} for subtracting natural contamination, but since it is the least abundant natural isotope, the accuracy of the subtraction is reduced, and this was used only as a check.

Similarly, in the Nd fraction and Eu fraction, we have used the same procedure. Nd^{142} and Eu^{151} are both shielded from the β chain, and they can be used for natural contamination correction (chain position is 2.87 for Pr^{142} and 3.51 for Eu^{151} in the same bombardment). The only shielded isotopes of cerium are Ce^{136} and Ce^{138}, but their natural abundances are too small for accurate correction purposes. In addition, the natural barium present in most samples, makes observation of Ce^{136} and Ce^{138} difficult. Usually the Ce fraction was matched to the Nd fraction by extrapolation of the yield-mass curve obtained from the Nd fraction back to mass 140. Using the extrapolated value for the Ce^{140} yield, and the data on absolute yields from the spike sample, we substituted this in the Ce fraction, to determine the yields for Ce^{142} and Ce^{144}. The Ce^{144} point must match the Nd^{144} point (after corrections for decay and growth respectively) as a check on the correctness of the extrapolation. Occasionally, the yield at Ce^{144} was used to match the Nd^{144} yield, and from this we obtained the yields of both Ce^{140} and Ce^{142}.

---

*Chain position is the difference between the charge of the isotope Z and the most probable charge of that mass chain Z_p.

In some cases, the independent yield of the isotope of higher Z than the stable isotope in a β chain was not negligible. Then corrections had to be made in order to get the total chain yield. For instance, in the mass-150 chain in the target mentioned before, the total chain yield should be the sum of Nd^{150} and Sm^{150} (independent yield of Pm^{150}). (This will be done when the absolute number of atoms is obtained, i.e., after calculation from the spiked sample). In case the independent yield could not be measured directly, the estimations were made from our charge-distribution correlation. Especially in the 45.7-Mev helium-ion bombardment of U^{235}, several measured yields were only cumulative yields rather than total chain yields. (Cumulative yields represent the accumulation of all the independent yields up to that isotope in this given chain, but total chain yields refer to the total mass chain). For example, Sm^{148} and Sm^{150} were added to Nd^{148} and Nd^{150} respectively to give the chain yields. In the decay correction for mass 144 and mass 147, the independent yields of Pr^{144} and Pm^{147} had to be considered. All these corrections were of the order of a few percent at the most.

In the thermal-neutron irradiation of U^{235}, the contamination level was negligible compared with the amount made in the reaction. As for the contributions due to neutron capture, corrections were made similar to that of Inghram et al.[5] Again these corrections were very small ($\ll 1\%$).

In the high-energy bombardment (730-Mev protons), the corrections were serious. In the first place, the amount of material made in the reaction was smaller on account of the lower beam, and the contamination level was higher owing to a large target size. Since both neutron-excess and neutron-deficient isotopes were made as primary fission products, there was in general no shielded isotopes that could be used to correct for natural contamination in any element. Assumptions had to be made for each fraction. These are discussed in a later section.

Spiked Sample

Once the ratios between isotopes within an element have been established, only one yield (number of atoms rather than cross section in millibarns) is needed to calculate the relative yields of all the

others. This can be achieved by measuring the ratio of that isotope to the spiking isotope in the sample. From the amount of the spiked material added and the results for the unspiked sample, the yield can be determined for all isotopes measured in the unspiked sample.

The isotopic yields thus obtained from different elements were put together and constitute the yield mass curve (or mass-distribution curve) in this region, independent of any assumptions and without the use of radiochemical data. Of course the absolute yield per fission is not determined by this process because of the possible inhomogeneity of the target thickness and the uncertainty in beam measurement. However, the estimation does show reasonable agreement with radiochemical data.[22]

Independent Yields

For Medium-Energy Bombardments (24- and 45.7-Mev Helium Ions)

Some of the independent yields were measured incidental to the total chain yields. For example, Pm^{150} (observed as Sm^{150}) and Eu^{154} were both measured in the 45.7-Mev helium-ion bombardments of U^{238} and U^{235} along with the chain yield measurements. The independent yields of several cesium isotopes and a couple of rubidium isotopes were also measured. The treatment of these data was somewhat different from the chain yield data. First, since we are interested only in the fractional chain yield,* spiking the sample is not of absolute necessity; in addition, there is only one stable isotope of cesium (Cs^{133}), spiking can be possible in this case only with a separated long-lived isotope (e.g., Cs^{137}), and we did not have a pure isotope of this type available.

Some assumptions were made in order to calculate the fractional chain yields. In the 24-Mev helium ion bombardment of U^{238}, the yields of both Cs^{135} and Cs^{137} were total chain yields. These two yields were

*"Fractional chain yield" used in this work differs from the independent yield in that the former is independent yield expressed as a fraction of the total chain yield of that mass chain; however, the latter can be in any units.

extrapolated to Cs^{134} (which was the lightest independent yield measured in this element), in order to obtain the total chain yields for Cs^{134} and Cs^{136}. The slope and the shape of the smooth curve chosen were determined by the extrapolation of the yield-mass curve obtained in the last section, and by comparing with the data of Vandenbosch et al.[22]

For the 45.7-Mev bombardments, the Cs^{135} and Cs^{137} yields were corrected for the small independent yields of the barium isotopes in the same chain. These yields were evaluated by using our charge-distribution correlation (discussed later). The fractional chain yields were then calculated as before.

For the rubidium fraction, Rb^{85} was assumed to be natural contamination. This may not be quite true, because Kr^{85m} may contribute some yield from the β chain, and therefore the subsequently calculated chain yield of Rb^{87} is a lower limit. (No correction was required for the independent yield of Sr^{87}). Since the natural level is higher than the amount made in the reaction (by a factor of about 4 for Rb^{85}, by estimation), and Rb^{85} is the major isotope, the true yield of Rb^{87} is not greater by a large amount. (Using the ratio of β^- to IT for Kr^{85m} from Strominger et al.,[55] and even assuming all the β^- chain goes through Kr^{85m}, one would find the correction to be only 15%). The slope of the yield-mass curve in this region was obtained by reflection, since the chain yields on the heavy wing of the yield-mass curve were known from this work on chain yields of the rare earths. (The point of reflection depends on the number of neutrons boiled off; this latter is discussed later).

For High-Energy Bombardments (730-Mev Protons and 100-Mev Carbon Ions)

Several of the cesium isotopes are shielded on both the neutron-excess and the neutron-deficient side, such as Cs^{132}, Cs^{134}, and Cs^{136}. Therefore no corrections of any kind need be made for these isotopes. Cs^{129}, Cs^{131}, and Cs^{135} are shielded on one side and the other side is partially shielded by fairly long-lived isotopes. Two runs separated by a known decay time were made in order to calculate these independent yields. Cs^{127} and Cs^{137} are both cumulative yields (or half-chain

yields). We estimated the percentage of the independent yield in the partial chain up to that point, by using the shape of the independent yield distribution in cesium obtained directly, and using the constant charge-to-mass ratio to determine the position of maximum for the adjacent elements, together with the slope of the yield-mass curve from 340-Mev proton work at this region (the slope of the yield-mass curve in this region should not change very much from 340 Mev to 730 Mev). The uncertainty for the Cs^{127} measurement is greater than that of Cs^{137}; the uncertainty for the Cs^{137} measurement amounts to 15 to 20%. However, the rapid drop on the light-mass side of the raw data indicates that it cannot be too far off.

For the Rb fraction, Rb^{84} and Rb^{86} are doubly shielded and Rb^{83} is singly shielded. The same technique as for Cs^{127} and Cs^{137} was used to estimate the independent yield of Rb^{83}.

For the Hilac bombardment (100-Mev carbon ions), independent yields were obtained for Cs^{132}, Cs^{134}, and Cs^{136}. Two runs were made for Cs^{131} and Cs^{135}, but the second run was unsuccessful for Cs^{131}. Its independent yield was therefore not determined. It would, however, not be much lower than the observed yield because of the sharp drop in yields on the light-mass side. Cs^{137} was again corrected by using the technique described in the preceding paragraph.

Chain Yields for Bombardment of U^{238} with 730-Mev Protons

As mentioned in the last section, there is no unambiguous way to correct for the natural contamination in high-energy fission. Therefore, certain assumptions were made to estimate the amount of natural contamination. However, these assumptions were not purely arbitrary. The distribution of independent yields determined for cesium isotopes, which are free from contamination, gives some indication of the distribution of isotopes of any element.

In the Ce fraction, we first assumed that the yield of mass 140 should be twice the yield of mass 142, because Ce^{140} is almost a total chain (the yields were measured a few months after the bombardment), and Ce^{142} includes only that part of the chain yield from the neutron-excess

isobars. In the Nd fraction, the yield of mass 145 was first assumed to be the same as that of mass 146. The approximation was based on the broad distribution of the independent yields which extends to isotopes very rich in neutrons, as observed in the Cs fraction. In addition, of the uncorrected observation of the Nd fraction, both Nd^{142} and Nd^{150} were in sizable abundance, yet they were not in the natural composition ratio. Thus the only reasonable explanation is that the distribution is quite broad. For the Sm fraction, we assumed that mass 151 has the same cumulative yield as mass 152, considering the 9.2-hr Eu^{152m} contributes something to Sm^{152} to even out the yields over what one would expect from the cesium data. After the first set of assumptions was made, separate corrections were made for the natural contamination, and from the results for the spiked samples, absolute numbers of atoms were obtained. Between mass 140 and mass 150, the total chain yields were obtained by summing all the yields of a given mass chain from the three elements. Of course decay corrections were made where necessary; again the assumptions made were based on the independent yield distribution here. Further small adjustments to the original approximations were made until a smooth yield-mass curve was obtained for the corrected total chain yields. The yields of Sm^{151}, Sm^{152}, and Sm^{154} were not corrected to total chain yields, because an accurate result would require measurements of the Eu fraction and the Gd fraction. Therefore these yields served as lower limits to the total chain yield.

Decay Correction for Eu^{155} and the Proposed New Half Life for Eu^{155}

Measurements of the yield of 1.7-yr Eu^{155} always gave mass 155 a total chain yield greater than the smooth yield-mass curve by 10 to 15% (after the decay correction). We first considered two possible explanations: a contribution from LaO^{+} in the mass spectrometer, which appears at the same mass number*; or a real change of shape of the yield-mass

*This is the case in which the mass peak may be ambiguous. But the ability of the mass spectrometer to differentiate among elements helped us to solve the problem.

curve in this region. However, this result seemed to reproduce with different target and runs. Another explanation was then considered--an incorrect half life for Eu^{155}. We first rechecked one of our old samples, and found the decay followed a half life of roughly 4 years. Then we reanalyzed a sample of Eu^{155} which had been previously analyzed 3 years earlier. We observed a half life of 4.25 years based on decay of three points over a period of three years. The decay of this sample is still being followed in this laboratory in order to give a better half life determination. The half life for Eu^{155} used throughout this work was 4.25 yr.

RESULTS*

Chain Yields

The chain yields for fission of U^{238} induced by 45.7-Mev and 24-Mev helium ions and of U^{235} induced by 45.7-Mev helium ions are tabulated in Tables II, III, and IV. The "Observed" columns in these tables are the results calculated from both the unspiked and the spiked data. The yields are all relative to Nd^{143}. We have measured the absolute number of atoms produced in each bombardment, and for convenience in comparison, the yields of Nd^{143} were normalized to unity in all cases. Corrections for the U^{238} bombardments are mainly decay corrections for partial chains. Ce^{144} data were given to show the matching of the Ce fraction and the Nd fraction, and also the reasonableness of the extrapolation to mass 140. These results are shown in Figs. 2, 3, and 4.

The U^{235} sample was 93.2% U^{235} and 6.8% U^{238}, and since the slope and the shape of the yield-mass curves for the two isotopes are not exactly the same, corrections of the yields due to isotopic composition were made in the 45.7-Mev helium-ion bombardment of U^{235} by using our U^{238} results. These corrections were made on an absolute basis, correcting

*The limits of error throughout this section are purely statistical; they are all standard deviations of the measurements.

Table II

Total chain yields for fission of U^{238} induced by 45.7-Mev helium ions

Nuclides	Observed	Corrected[a]	
Ce^{140}	1.27±0.01[b]	1.27±0.01	
Ce^{142}	1.15±0.01	1.15±0.01	
Nd^{143}	1.00±0.02	1.00±0.02	
Ce^{144}	0.54±0.01	0.92±0.02	0.90±0.03[c]
Nd^{144}	0.21±0.01	0.88±0.04	
Nd^{145}	0.81±0.02	0.81±0.02	
Nd^{146}	0.67±0.01	0.67±0.01	
Sm^{147}	0.04±0.015	0.58±0.02	
Nd^{148}	0.52±0.01	0.52±0.01	
Sm^{149}	0.43±0.01	0.43±0.01	
Nd^{150}	0.37±0.009	0.38±0.01	
Sm^{150}	0.0125±0.001		
Sm^{151}	0.312±0.010	0.312±0.010	
Sm^{152}	0.259±0.009	0.259±0.009	
Eu^{153}	0.218±0.005	0.218±0.005	
Sm^{154}	0.160±0.003	0.160±0.003	
Eu^{155}	0.116±0.003	0.125±0.003	

[a] All the decay corrections in this work were made by using the first choice of the half lives listed in Table of Isotopes by Strominger et al.[55] except for 4.25-yr Eu^{155}.

[b] This is an extrapolated value. The extrapolation was made so that the amount of natural contamination and the amounts of Ce^{142} and Ce^{144} made in the reaction can be determined, by using the results of the spiked sample.

[c] This is the average of the results from Ce^{144} and Nd^{144}. Notice that the corrected value is not equal to the sum of Ce^{144} and Nd^{144} in the "Observed" column, since there was a time interval between the chemical separation and running the samples in the mass spectrometer.

Table III

Total chain yields for fission of U^{238} induced by 24-Mev helium ions

Nuclides	Observed	Corrected	
Ce^{140}	1.35±0.03[a]	1.35±0.03	
Ce^{142}	1.18±0.03	1.18±0.03	
Nd^{143}	1.00±0.03	1.00±0.03	
Ce^{144}	0.49±0.02	0.84±0.03	0.86±0.04
Nd^{144}	0.36±0.02	0.88±0.05	
Nd^{145}	0.76±0.02	0.76±0.02	
Nd^{146}	0.64±0.02	0.64±0.02	
Sm^{147}	0.076±0.0035	0.57±0.03	
Nd^{148}	0.51±0.02	0.51±0.02	
Sm^{149}	0.39±0.01	0.39±0.01	
Nd^{150}	0.35±0.01	0.35±0.01	
Sm^{151}	0.288±0.003	0.288±0.003	
Sm^{152}	0.222±0.001	0.222±0.001	
Eu^{153}	0.164±0.005	0.164±0.005	
Sm^{154}	0.127±0.004	0.127±0.004	
Eu^{155}	0.094±0.003	0.105±0.003	

[a]Extrapolated value.

Table IV

Total chain yields for fission of U^{235} induced by 45.7-Mev helium ions

Nuclides	Observed	Corrected for decay and chain yields	Corrected for isotopic composition of target
Ce^{140}	1.12±0.01	1.12±0.01	1.14±0.01
Ce^{142}	1.03±0.01		
Nd^{142}	0.0066[a]	1.04±0.01	1.05±0.01
Nd^{143}	1.00±0.02	1.00±0.02	1.00±0.02
Ce^{144}	0.57±0.01[b]		
Nd^{144}	0.27±0.004	0.89±0.02[a]	0.89±0.02
Nd^{145}	0.77±0.01	0.77±0.01	0.77±0.01
Nd^{146}	0.65±0.01	0.65±0.01	0.65±0.01
Sm^{147}	0.035±0.004	0.53±0.06[a]	0.54±0.06
Nd^{148}	0.454±0.007		
Sm^{148}	0.007±0.001	0.461±0.007	0.464±0.007
Sm^{149}	0.380±0.012	0.380±0.012	0.383±0.012
Nd^{150}	0.270±0.009		
Sm^{150}	0.053±0.003	0.323±0.010	0.326±0.010
Sm^{151}	0.263±0.009	0.263±0.009	0.266±0.009
Sm^{152}	0.200±0.004	0.200±0.004	0.203±0.004
Eu^{153}	0.171±0.003	0.171±0.003	0.174±0.004
Sm^{154}	0.116±0.003		
Eu^{154}	0.006±0.0003	0.122±0.003	0.124±0.004
Eu^{155}	0.098±0.002	0.104±0.002	0.105±0.002

[a] Assumed independent yields from the charge distribution curve obtained in this work.

[b] Matched value to Nd^{144}

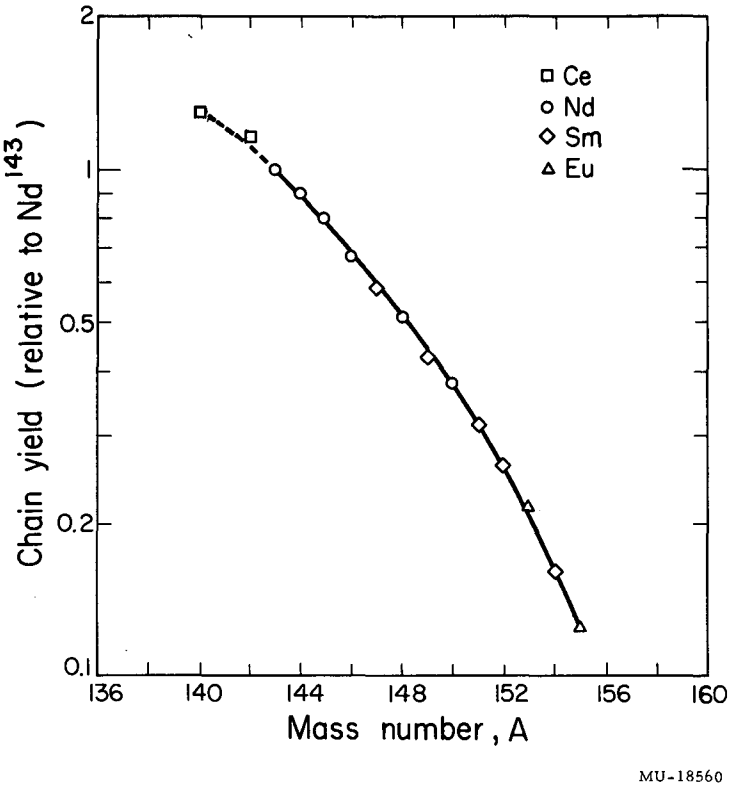

Fig. 2. Yield-mass curve for fission of U^{238} induced by 45.7-Mev helium ions.

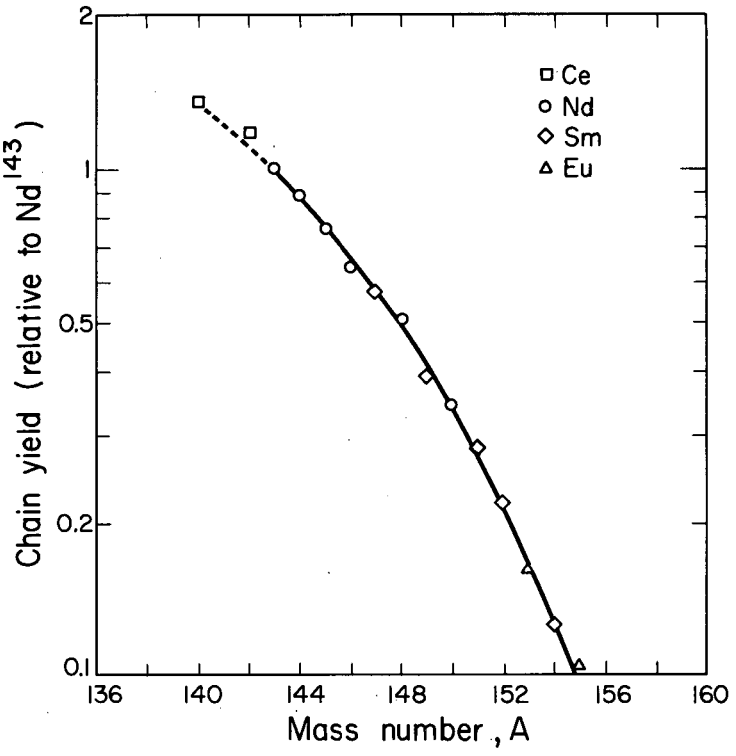

Fig. 3. Yield-mass curve for fission of U^{238} induced by 24-Mev helium ions.

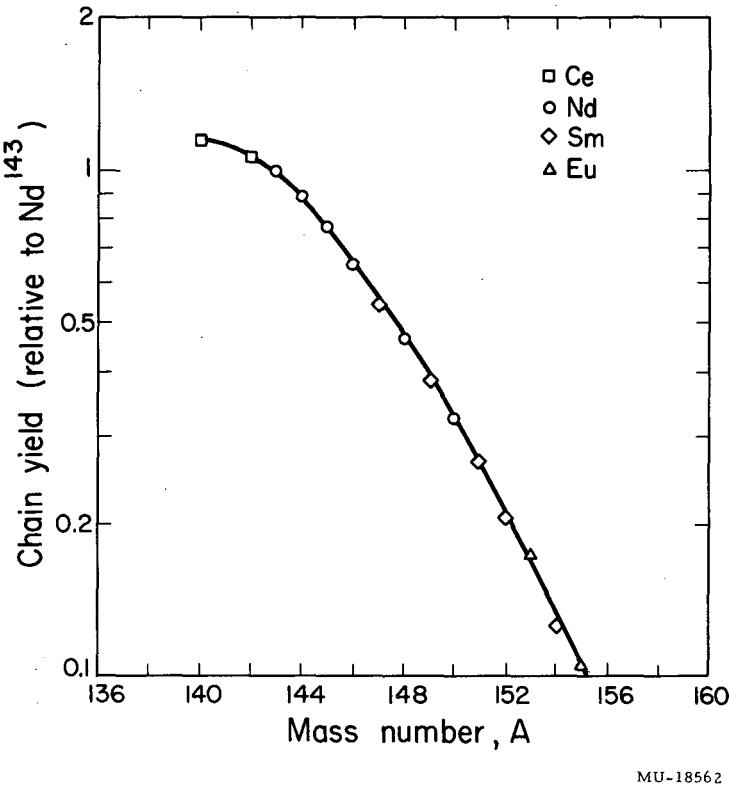

Fig. 4. Yield-mass curve for fission of U^{235} induced by 45.7-Mev helium ions.

for total integrated beam in each target. The correction for U^{235} in natural uranium was negligible because only 0.7% U^{235} was present. Also, independent yield corrections were made in some chains, since the primary fission fragments of U^{235} are closer to the line of stability than those of U^{238} with the same excitation energy. The corrections for the U^{238} target again were negligible; but for the U^{235} target, sometimes it amounted to a few percent.

The total chain yields for thermal-neutron fission of U^{235} are given in Table V. The corrections are both for decay and for neutron capture. Since the neutron flux used was rather low, and the irradiation time was rather short, no capture correction exceeded 1%. The results are plotted in Fig. 5.

The total chain yields for fission of U^{238} induced by 730-Mev protons are presented in Table VI. We have discussed before the assumptions made to correct for natural contaminations in this case. The columns given as "Observed" are the compositions after these contaminations were subtracted. Note that masses 151, 152, and 154 remained uncorrected, and they are thus lower limits for the respective chains. The results are shown in Fig. 6.

Fractional Chain Yields of Shielded Isotopes

The fractional chain yields of several shielded isotopes for fission of U^{238} and U^{235} with 45.7-Mev and 24-Mev helium ions are given in Tables VII, VIII, IX, and X. The "Corrected" columns under "Independent yields" were corrected only for decay. Then the corrected independent yields were converted to the fractional chain yields. Because U^{235} targets gave much higher independent yields than the corresponding U^{238} targets, the corrections of the yields due to isotopic composition were quite important even for U^{238} (natural uranium was used here; the 0.7% of U^{235} can change the independent yields considerably). The last column gives final results for fractional chain yield used in the discussion of charge distribution.

Table V

Total chain yields for fission of U^{235} induced by thermal neutrons

Nuclides	Observed	Corrected
Ce^{140}	1.05±0.01	1.05±0.01
Ce^{142}	1.00±0.01	1.00±0.01
Nd^{143}	1.00±0.01	1.00±0.01
Ce^{144}	0.664±0.016[a]	
Nd^{144}	0.190±0.004	0.90±0.02[b]
Nd^{145}	0.66±0.004	0.66±0.004
Nd^{146}	0.50±0.005	0.50±0.005
Sm^{147}	0.022±0.0002	0.38±0.004[b]
Nd^{148}	0.282±0.002	0.282±0.002
Sm^{149}	0.185±0.001	0.186±0.001[c]
Nd^{150}	0.1095±0.0019	
Sm^{150}	0.00023±0.00001	0.110±0.002
Sm^{151}	0.070±0.0005	0.070±0.0005
Sm^{152}	0.045±0.0003	0.045±0.0003
Eu^{153}	0.0276±0.0008	0.0276±0.0008
Sm^{154}	0.0125±0.00012	0.0125±0.0001
Eu^{155}	0.00519±0.00015	0.00544±0.00016[d]

[a] Matched value of Nd^{144}.

[b] Corrected for decay.

[c] Corrected for neutron capture.

[d] Corrected for both decay and neutron capture.

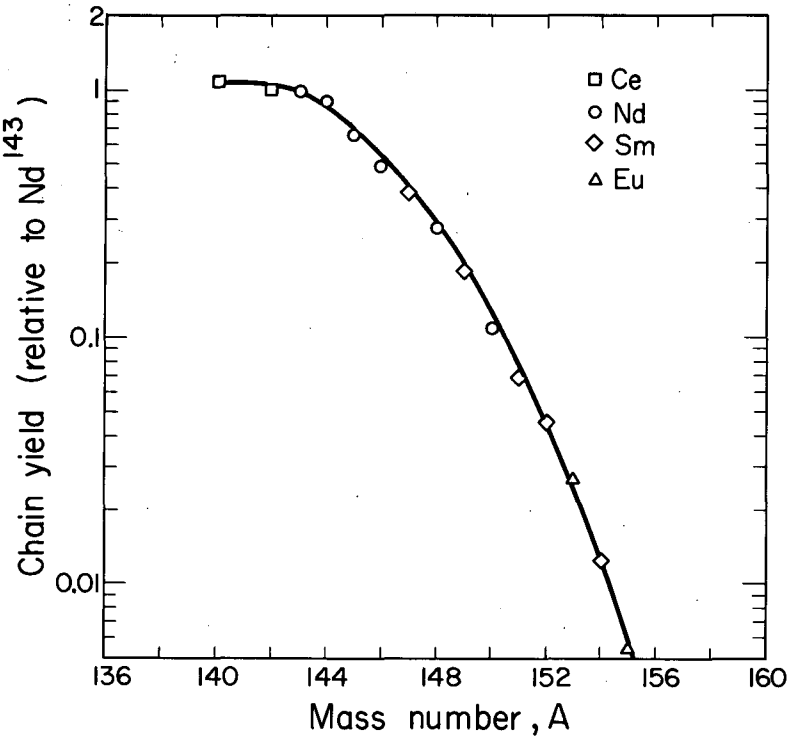

Fig. 5. Yield-mass curve for fission of U^{235} induced by thermal neutrons.

Table VI

Total chain yields for fission of U^{238} induced by 730-Mev protons

	Ce fraction		Nd fraction		Sm fraction		
Mass	Observed	Corrected	Observed	Corrected	Observed	Corrected	Total
140	1.44±0.06	1.44±0.06					1.44±0.06
142	0.71±0.03	0.71±0.03	0.39±0.06	0.39±0.06			1.10±0.08
143			0.88±0.09	1.00±0.11[a]			1.00±0.11
144	0.39±0.02	0.39±0.02	0.50±0.07	0.50±0.07	0.04±0.003	0.04±0.003	0.93±0.008
145			0.59±0.08	0.59±0.08	0.06±0.004	0.08±0.005	0.67±0.07
146			0.51±0.07	0.51±0.07	0.07±0.007	0.07±0.007	0.58±0.07
147					0.115±0.007	0.42±0.03[b]	0.42±0.03
148			0.27±0.04	0.27±0.04	0.10±0.008	0.10±0.008	0.37±0.04
149					0.27±0.02	0.30±0.02[c]	0.30±0.02
150			0.15±0.02	0.15±0.02	0.06±0.006	0.06±0.006	0.21±0.02
151					0.12±0.01[d]	0.12±0.01[d]	0.12±0.01[d]
152					0.12±0.01[d]	0.12±0.01[d]	0.12±0.01[d]
154					0.06±0.004[d]	0.06±0.004[d]	0.06±0.004[d]

[a] Assume the contribution from the neutron-deficient side is 15% of the total chain.

[b] Assume the contribution from the neutron-deficient side up to Sm^{147} is 20% of the 147 chain.

[c] Assume the contribution on the neutron-deficient side is 20% of the chain.

[d] These are cumulative yields rather than total chain yields, since the data were left uncorrected on account of large uncertainties.

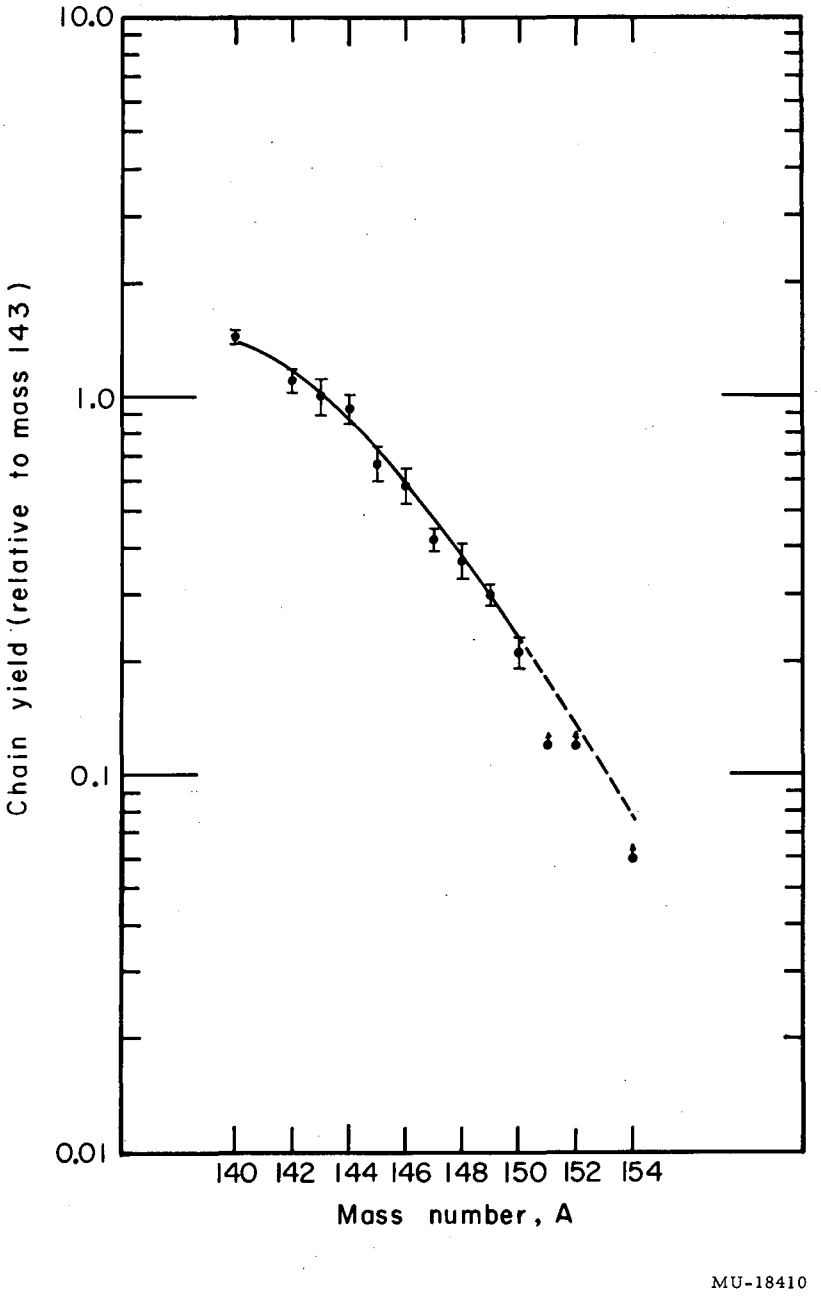

Fig. 6. Yield-mass curve for fission of U^{238} induced by 730-Mev protons.

Table VII

Fractional chain yields for fission of U^{238} induced by 45.7-Mev helium ions

Nuclides	Independent yields[a] Observed	Corrected	Fractional[b] chain yields	Corrected for isotopic composition of target
Rb^{84}	<0.00007	<0.00007	<0.00012	<0.00011
Rb^{86}	0.0019	0.00212	0.00257	0.00243±0.00005
Cs^{131}	0.00014	0.00016	0.00012	0.000097±0.000007
Cs^{132}	0.00105	0.00116	0.00093	0.00081±0.00002
Cs^{134}	0.0394	0.0394	0.0320	0.0309±0.0002
Cs^{136}	0.1823	0.1945	0.1691	0.1671±0.0040
Pm^{150}	0.0293	0.0293	0.0328	0.0318±0.0009
Eu^{154}	0.0029	0.00303	0.00413	0.00374±0.0002

[a]Compared with the adjacent chain yields, e.g., Rb^{87}, Cs^{137}, Sm^{149} (Sm^{150} was measured for the independent yield of Pm^{150}), and Eu^{153}.

[b]Fractional chain yield is the ratio of the independent yield to the total chain yield of that particular mass number.

Table VIII

Fractional chain yields for fission of U^{238} induced by 24-Mev helium ions

Nuclides	Independent yields[a] Observed	Corrected	Fractional chain yields	Corrected for isotopic composition of target
Cs^{134}	0.00611	0.00611	0.00596	0.00575±0.00040
Cs^{136}	0.0248	0.0303	0.0310	0.0292±0.0020

[a]Compared with Cs^{135} chain yield.

Table IX

Fractional chain yields for fission of U^{235} induced by 45.7-Mev helium ions

Nuclides	Independent yields[a] Observed	Independent yields[a] Corrected	Fractional chain yields	Corrected for isotopic composition of target
Rb^{84}	0.00081	0.00088	0.00147	0.00157±0.00004
Rb^{86}	0.0145	0.0182	0.0217	0.0231±0.0008
Cs^{131}	0.0166	0.0227	0.00355	0.0038±0.00009
Cs^{132}	0.0629	0.1022	0.0164	0.0175±0.00064
Cs^{134}	1.000	1.000	0.1730	0.1834±0.0023
Cs^{136}	1.759	2.204	0.4247	0.4435±0.0085
Pm^{148}	0.0179	0.0179	0.0147	0.0158±0.0007
Pm^{150}	0.1393	0.1393	0.1637	0.1733±0.0110
Eu^{154}	0.0350	0.0366	0.0465	0.0496±0.0024

[a]Except for Cs isotopes, all independent yields in this column are compared with the adjacent chain yields: Rb^{87}, Sm^{149}, and Eu^{153}. Cs isotopes are compared with Cs^{134} in arbitrary units.

Table X

Fractional chain yields for fission of U^{235} induced by 24-Mev helium ions

Nuclides	Independent yields[a] Observed	Independent yields[a] Corrected	Fractional chain yields	Corrected for isotopic composition of target
Cs^{132}	0.0011	0.0017	0.00156	0.00167±0.00009
Cs^{134}	0.0355	0.0355	0.0338	0.0359±0.0006
Cs^{136}	0.2116	0.2641	0.2673	0.2847±0.0060

[a]Compared with Cs^{135} chain yield.

Table XI

Independent yields for fission of U^{238} induced by 730-Mev protons

Nuclides	Independent yields		Average
	Observed	Corrected	
Rb^{83}	0.275±0.006	0.226±0.005[a]	
Rb^{84}	0.439±0.005	0.473±0.005	
Rb^{86}	0.876±0.009	1.000±0.010	
Cs^{127}	0.500±0.022[b]	0.375±0.016[a]	
Cs^{129}	1.010±0.009	0.744±0.022	
	1.377±0.041		
Cs^{131}	1.039±0.016	1.082±0.013	
	0.964±0.010		
Cs^{132}	1.001±0.042	1.058±0.044	1.083±0.028
	0.765±0.008	1.108±0.011	
Cs^{134}	1.000±0.025	1.000±0.025	
Cs^{135}	1.084±0.015	0.974±0.013	
	3.433±0.043		
Cs^{136}	0.894±0.037	0.917±0.038	0.925±0.025
	0.777±0.010	0.933±0.012	
Cs^{137}	2.464±0.059	0.870±0.021[a]	

[a]Corrections were made according to the charge distribution along the mass chains 83, 127, and 137, using the mass distribution along the Cs fraction obtained in this work.

[b]Because of rather short half life of Cs^{127}, decay corrections had to be made during the mass spectrometer run, therefore the number given has already been corrected for decay.

For the 730-Mev proton fission of U^{238}, the Cs^{129}, Cs^{131}, and Cs^{135} can be determined only by two different runs differing in decay time. Therefore data from both runs are given under the "Observed" column of Table XI, and the independent yields are given under the "Corrected" column. For Cs^{132} and Cs^{136}, decay corrections were made separately for each bombardment and the average of the two was taken. Both the rubidium and the cesium results are plotted on Fig. 7.

The short bombardments with 100-Mev carbon ions on U^{238} gave the independent yields listed in Table XII and shown in Fig. 8. Two experiments were necessary to calculate the independent yields of Cs^{131} and Cs^{135} from the observed partial chain yields. Of these only the independent yield for Cs^{135} was reported. Because the observation of Cs^{131} was unsuccessful in one run, the Cs^{131} point is therefore left uncorrected. However, since the distribution of the independent yields is quite narrow, therefore the Cs^{131} datum probably is quite close to the independent yield.

Table XII

Independent yields for fission of U^{238} induced by 100-Mev carbon ions

Nuclides	Observed	Corrected
Cs^{131}	0.192±0.029	0.192±0.029[a]
Cs^{132}	0.383±0.034	0.399±0.036[b]
Cs^{134}	1.000±0.022	1.000±0.022
Cs^{135}	1.469±0.021 1.523±0.070	1.092±0.045[c]
Cs^{136}	0.944±0.027	0.974±0.029[b]
Cs^{137}	1.236±0.005	0.763±0.003[d]

[a] Uncorrected.

[b] Corrected for decay.

[c] Corrected for the decay of Xe^{135} in two runs.

[d] Correction according to the Text. The accuracy of this point is estimated to be 15 to 20%.

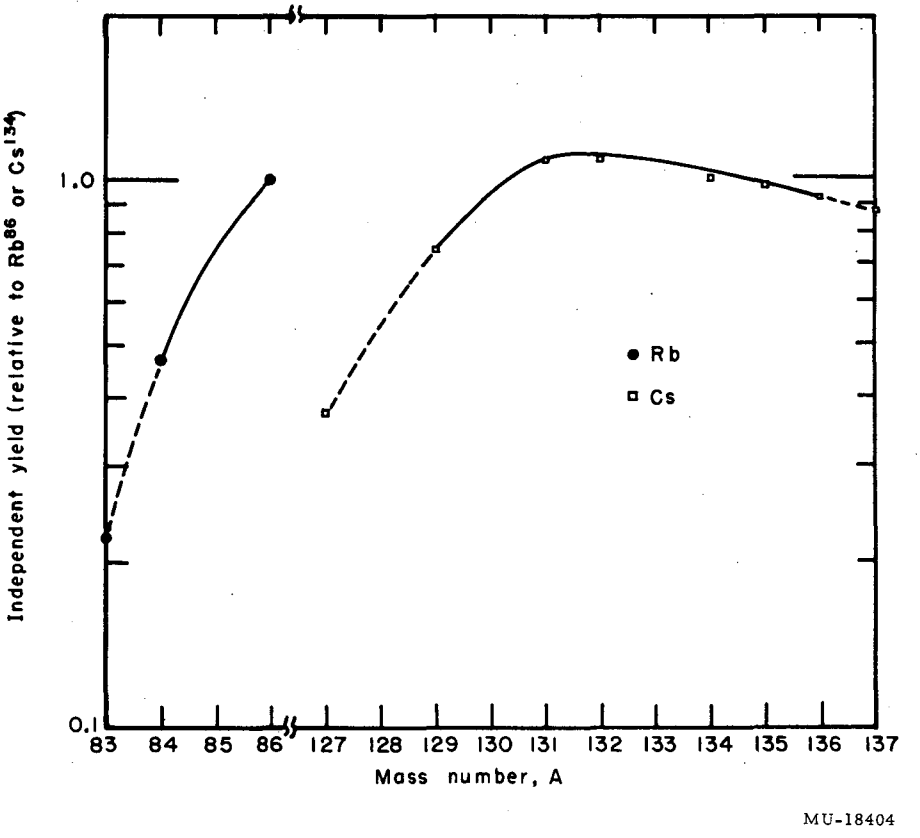

Fig. 7. Independent yield distributions of cesium fraction and rubidium fraction from fission of U^{238} induced by 730-Mev protons.

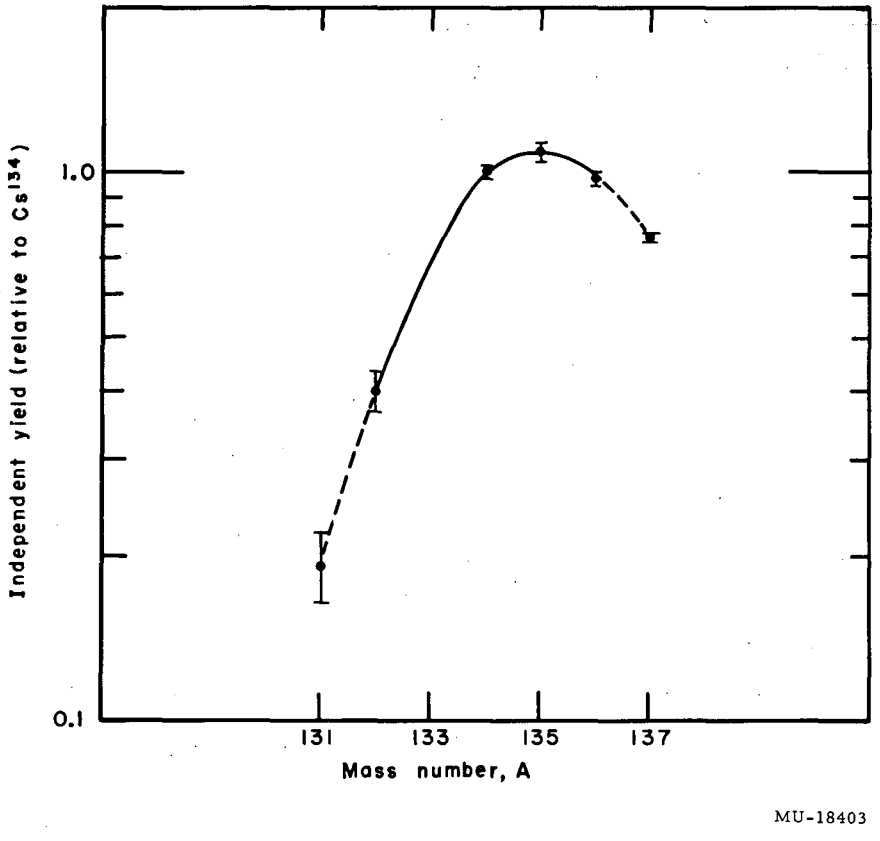

Fig. 8. Independent yield distribution of cesium fraction from fission of U^{238} induced by 100-Mev carbon ions.

DISCUSSION

Charge Distribution

The measured fractional chain yields were first correlated* by assuming that the charge distribution is the same as that reported by Wahl[56] for the thermal-neutron fission of U^{235}. This correlation was based on the assumption that the charge distribution at each mass should be very close to a Gaussian distribution.[30,46] We could then calculate the Z_P for these chains (by comparing the observed fractional chain yield with the empirical charge-distribution curve to get the chain position $Z - Z_P$ and thus Z_P). Coryell suggested that if one plots $(Z - 0.4A)$ versus A, most of the smooth A dependence will be removed, so that one can use the resulting expanded scale for $(Z - 0.4A)$ to see any real local effects.[57] Our data for the fission of U^{235} and U^{238} induced by 45.7-Mev helium ions are plotted separately, with the Z_P obtained above as Curve A and Curve B respectively, and they are compared with the thermal-neutron fission data compiled by Wahl[56] as Curve C, in Fig. 9. One can see that the prominent shell effect around A ~135 has definitely disappeared from the 45.7-Mev bombardments. The comparison of the relative positions between A ~135 and A ~ 150 in these cases clearly indicates this. Furthermore, one can compare these with $(Z - 0.4A)$ versus A by using the Z's of the odd-Z stable isotopes as an approximation to Z_A. The apparent parallel trend between these "Z_A's" and the thermal-neutron fission data is an indication that this kind of Z_A and the ECD rule are appropriate for neutron fission. However, this apparently does not fit the 45.7-Mev bombardments.

In order to demonstrate that the measured points are not by chance all equidistant from the most-stable-charge position, the comparisons are made in Fig. 10, where both $(Z - 0.4A)$ and $(Z_P - 0.4A)$ are plotted versus A. It shows that the measured points do cover a rather wide range of $Z - 0.4A$ and give a reasonable distribution.

---

*This has been suggested by Dr. J. M. Alexander.

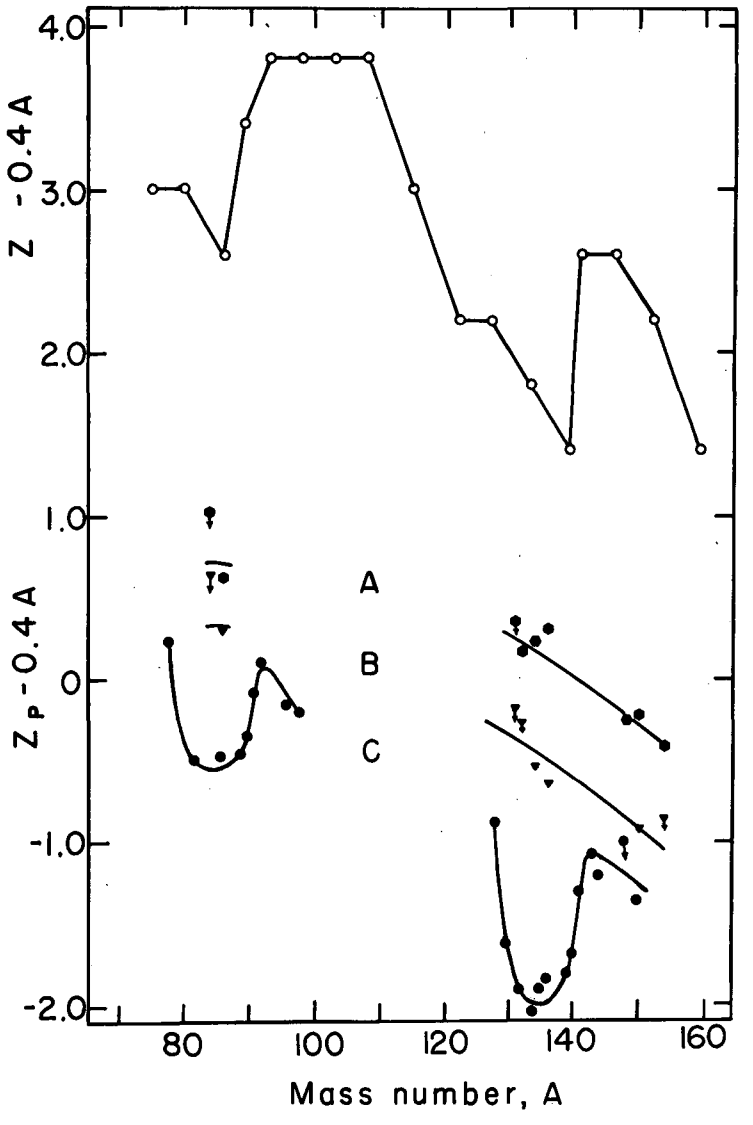

Fig. 9. Comparison of the empirical Z_p versus A on an expanded charge scale.

- ● U^{235} + 45.7-Mev helium ions (this work).
- ▼ U^{238} + 45.7-Mev helium ions (this work).
- ● U^{235} + thermal neutrons (from Wahl[56], except A = 150, which was measured in this work.)
- ○ Odd-Z stable nuclides.

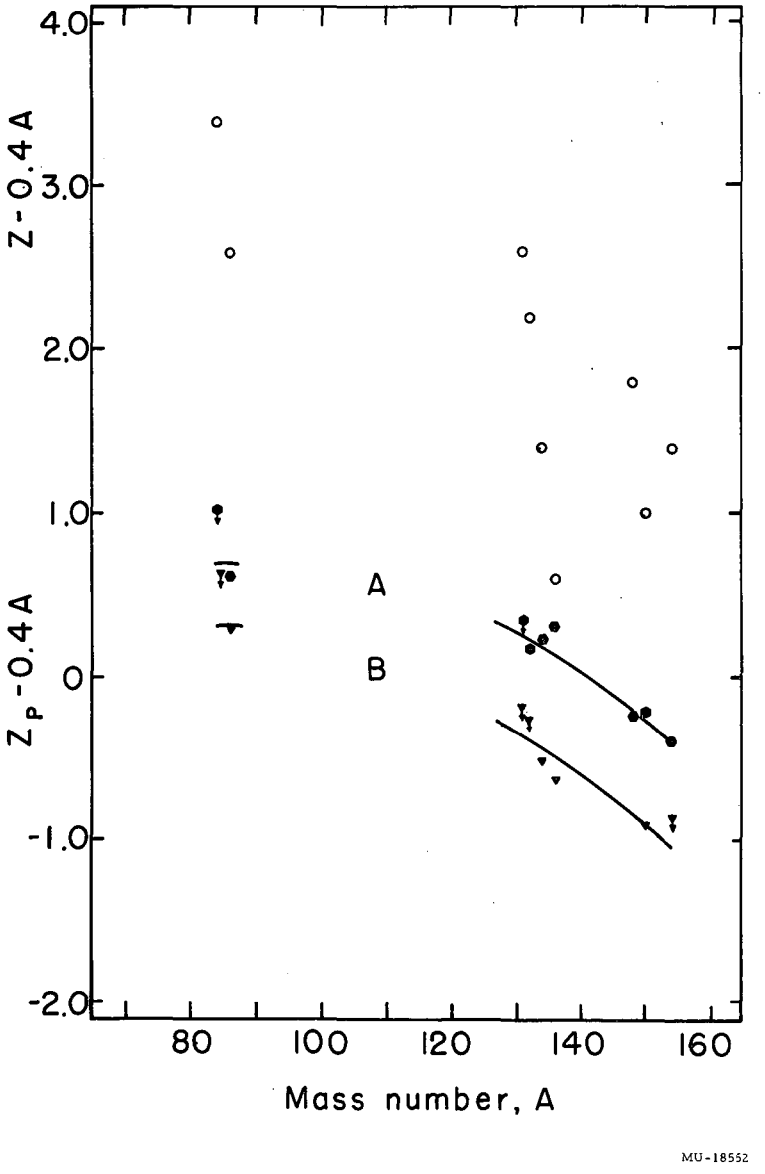

Fig. 10. The chain positions of the measured shielded nuclides on an expanded charge scale.

- ● U^{235} + 45.7-Mev helium ions.
- ▼ U^{238} + 45.7-Mev helium ions.
- ○ Z of the measured nuclides.

Incidentally, the scatterings shown on Fig. 9 can be accounted for in part by the difference in width between the actual distribution and Wahl's distribution. In fact, it is shown later that the actual distribution is broader than Wahl's, and is in agreement with Pate's observation.[58] The greatest effect would be on the low-yield isotopes, such as Rb^{84}, Cs^{131}, and Cs^{132}. Therefore upper-limit signs were used for these isotopes.

If one wants to look into this set of data further, one has to consider the assumptions and parameters involved. As a matter of fact, Wahl's empirical set of Z_p's[56] comprises at least two other assumptions:

(a) The charge distribution for a given mass chain is a smooth function varying with the nuclear charge Z, and is symmetric about the most probable charge Z_p of that mass chain in the particular fission process.

(b) The shape of the charge-distribution curve is invariant for all mass chains.

Fortunately these assumptions have been justified by many works, especially the recent results of Ferguson[59] as quoted from the thesis of Troutner,[60] which has shown that for the chains with masses 91, 139, and 140 the independent or cumulative yields of at least three members of each chain are in agreement with the normal charge-distribution curve of Wahl[56] for the thermal-neutron fission of U^{235}. This apparently substantiates the validity of these two assumptions.

When we later treat all the data in a single distribution curve, other assumptions come in automatically. That is, the charge distribution is assumed to be independent both of the targets used (U^{238} and U^{235}) and of the excitation energies involved in this work (~20 Mev and ~40 Mev). However, the reasonable fit of all the points on the same distribution indicates that these are fair assumptions.

Of course, in addition to these assumptions are the two major empirical rules (ECD and CCR) used in obtaining the most probable charge Z_p. And there are still several parameters that have to be considered.

(A) The total number of neutrons lost in the fission process. Thomas[23] suggested that this be given by

$$\nu = 2 + E_{ex}/8,$$

where E_{ex} is the excitation energy of the compound nucleus in Mev. The basis for this is that two neutrons are emitted for spontaneous fission[61] and an additional neutron is emitted for each 8 Mev of excitation. This has been generally accepted in much work on fission induced by charged particles in this energy range,[47,62] and is in agreement with Halpern's data for fission with fast neutrons.[63]

(B) The number of neutrons emitted before fission and the number of neutrons lost after fission. This can be determined by comparing with the experimental result of Vandenbosch et al.[22] of fission-spallation competition of uranium isotopes at this energy region.

(C) The distribution of postfission neutrons between the two fission fragments. In most cases, equal division between the two fragments is used.

(D) The most stable charge Z_A used. For all the charge-distribution work recently done, the Z_A values including the shell effect have invariably been used. Coryell has given the set of discontinuous Z_A values derived from the point of view of β energetics.[64] Recently, Grummitt and Milton have recalculated a new set of continuous Z_A values,[43] taking into account the shell effect from recent measurements and based on the nuclear mass data of Cameron.[65] Levy has obtained a set of Z_A values by using different parameters for different mass regions, considering the shell effect.[66]

In the next treatment of the data, we have calculated the number of neutrons lost according to Thomas' formula[23] (in the 45.7-Mev bombardments, $E_{ex} \sim 40$ Mev, therefore $\nu = 7$). We assumed that one neutron boiled off before fission in all cases in accordance with the experimental result of Vandenbosch et al.[22] The postfission neutrons were divided equally between the two fragments, and both Coryell's Z_A values[64] and those of Grummitt and Milton[43] were used for the ECD rule. All the points for both cases were scattered pretty badly. It would

look much better if the CCR rule were used. However, the integrated area under the best smooth curve drawn through the CCR points was much smaller than unity (~0.72).

Now if we go back to Fig. 9 and read off the smooth curve both from the light mass side (~85) and the heavy side (~150), assuming no charged particles emitted in these excitations, then in order to match both the charge and the mass of the two fragments to the fissioning nucleus, we find that the most probable number of neutrons emitted is ~5.5. Another way of looking at this would be plotting Z_P of the light and the heavy fragments as Wahl did,[56] assuming equal numbers of neutrons emitted from both fragments. It is obvious from Fig. 11 that $\nu = 5$ (solid points) gives a better linear correlation than $\nu = 7$ (open points). The arrow signs are due to the broader width of the actual distribution than the one taken from Wahl's paper,[56] used to construct Fig. 9.

Therefore in trying with five neutrons emitted for the 45.7-Mev bombardments, with all other parameters kept unchanged, we found that the CCR rule gave a fairly good fit with an integrated area very close to unity. It looked much better than the results with the ECD rule using either the Z_A due to Coryell or to Grummitt and Milton, as plotted on Fig. 12 and Fig. 13 respectively. The results for the CCR rule are shown in Fig. 14.

Up to this point, everything looked quite similar to what Gibson observed.[24] That is, the data fitted the CCR much better than the ECD. However, the fit for CCR was still not satisfactory, considering the accuracy of these measurements.

From Fig. 9, it is quite obvious that in the treatment of this set of data, it is irreconcilable to use either Coryell's or Grummitt and Milton's Z_A's for the ECD treatment (both Coryell's Z_A and those of Grummitt and Milton are very close to the Z_A obtained by drawing a curve through the odd-Z stable isotopes; the agreement is good to 0.1 or 0.2 charge unit). From another point of view, in the fitting of the ECD rule using Grummitt and Milton's Z_A values (Fig. 13), one can notice readily that the heavy fragments (Pm^{148}, Pm^{150}, and Eu^{154}) in general are much

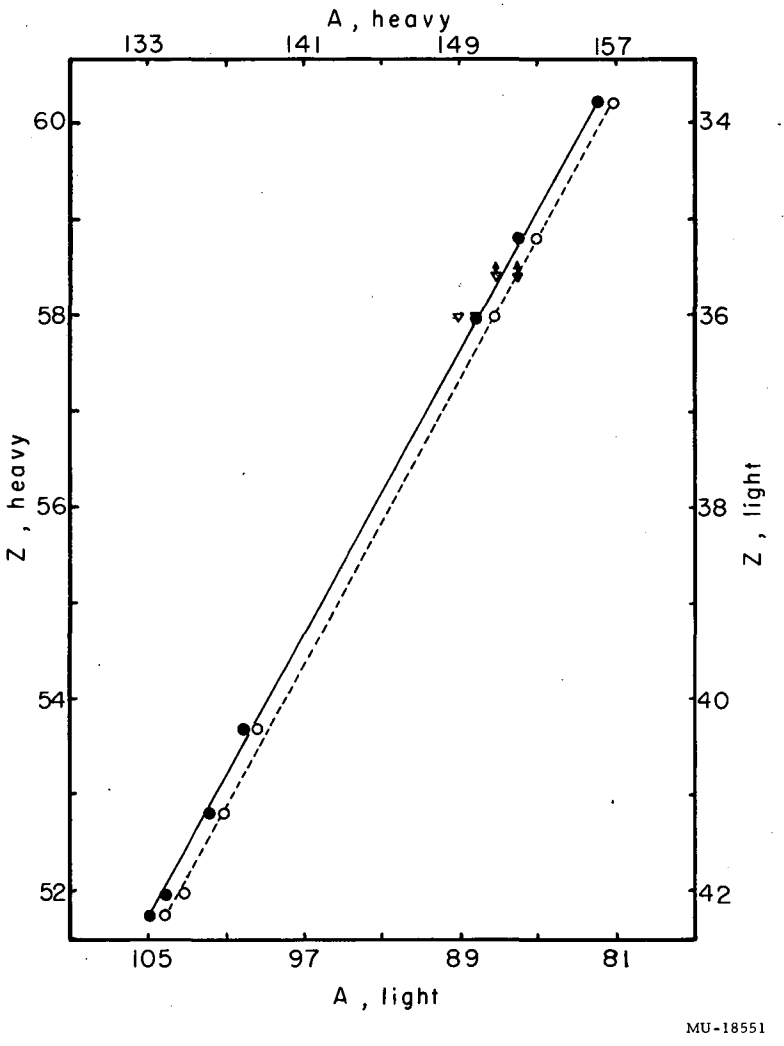

Fig. 11. The empirical Z_p function for fission of U^{235} induced by 45.7-Mev helium ions.

- ● Heavy fragments for $\nu = 5$.
- ▼ Light fragments for $\nu = 5$.
- ○ Heavy fragments for $\nu = 7$.
- ▽ Light fragments for $\nu = 7$.

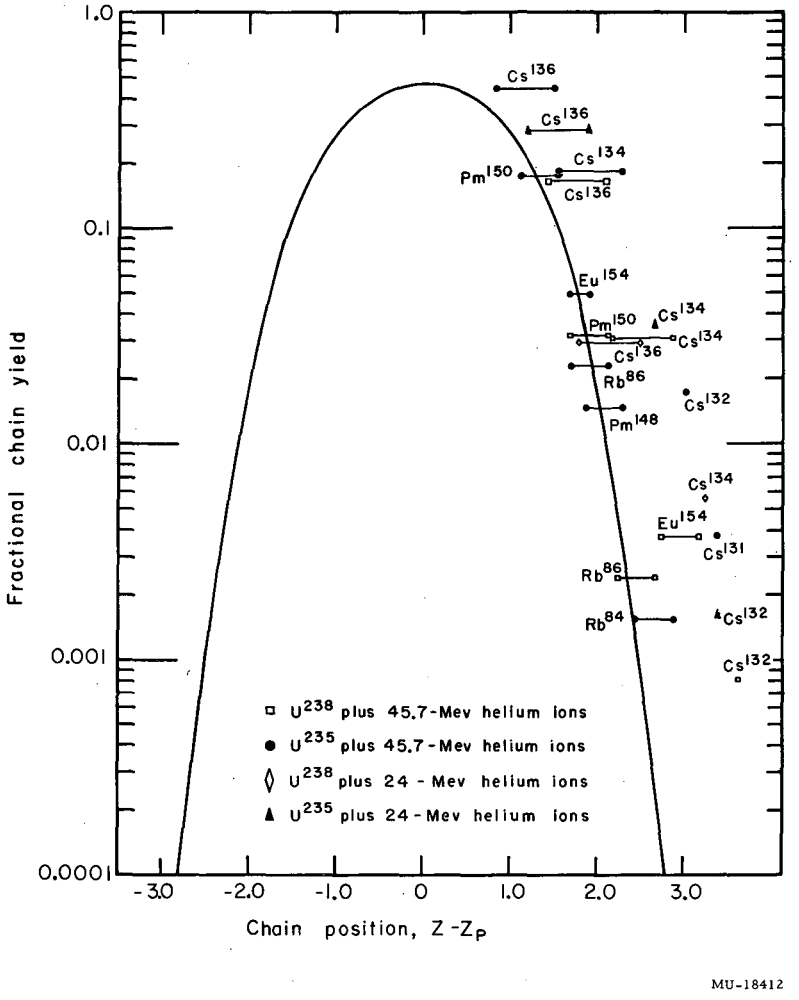

Fig. 12. Charge-distribution curve based on ECD rule and Coryell's Z_A values.[64] Smooth curve is that of Pappas[42] (for thermal-neutron fission of U^{235}).

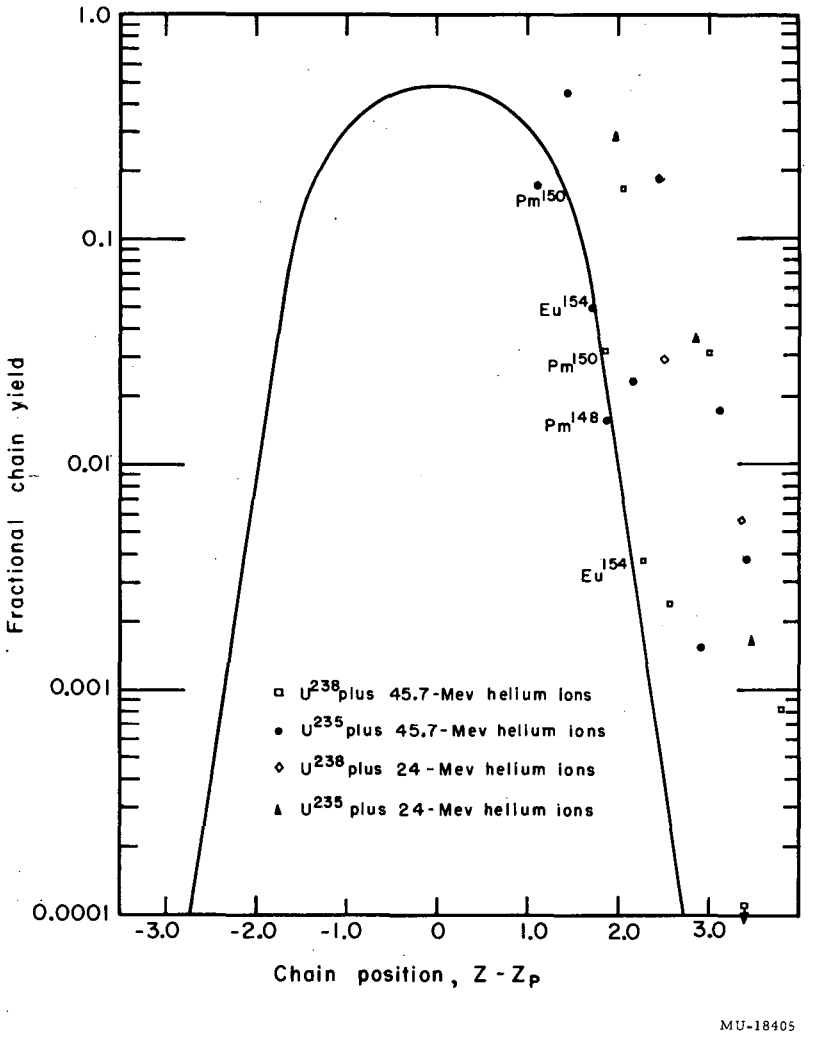

Fig. 13. Charge distribution curve based on ECD rule and Grummitt-Milton's Z_A values.[43] Smooth curve is that of Grummitt-Milton[43] (for thermal-neutron fission of U^{235}).

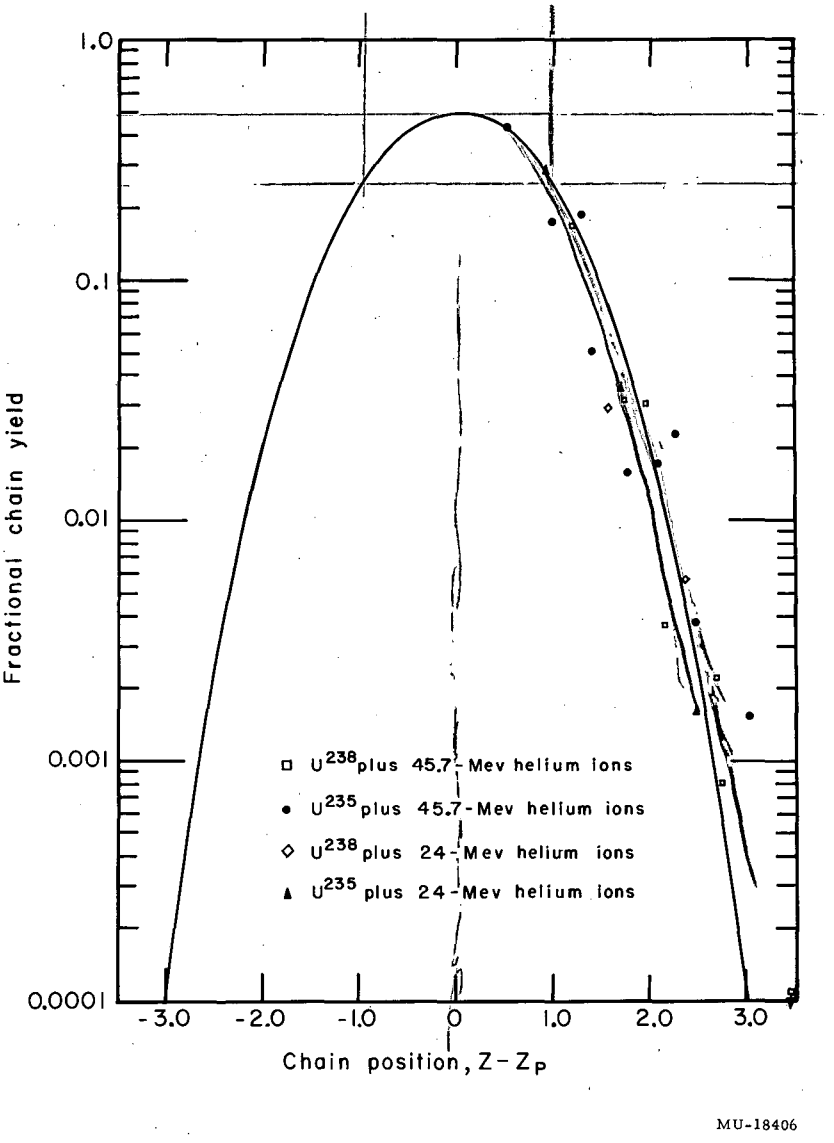

Fig. 14. Charge-distribution curve based on CCR rule.

lower than the lighter fragments (Rb^{84}, Rb^{86}, Cs^{131}, Cs^{132}, Cs^{134}, and Cs^{136}). In other words, somehow the chain positions for the lighter fragments should be shorter. If one looks at the Z_A-versus-A curves given on Fig. 15--the set of dashed lines, which is from Coryell's data, and the dashed-dotted curve, that of Grummitt and Milton--one finds that the discrepancy can be explained by the nonlinearity of the Z_A values.* For example, the heavy fragments (A ~ 150) have Z_A's on the upper portion, while their complementary fragments (A ~ 85) are on the lower portion of the Z_A curve; therefore in comparison with a linear Z_A function, the heavy fragments have higher Z_P's,** consequently shorter chain positions, and therefore the fractional chain yields are too low; the opposite is true for the lighter fragments. After comparing with Gibson's data again, we found that his data could be explained in the same manner (using the ECD treatment), as for Ag^{112}, the chain position of which is shorter than the others from the bombardments of Np^{237} with 45.7-Mev and 31.5-Mev helium ions.

Naturally the next thing to try was using a continuous and linear curve for Z_A versus A. The first one to come to hand was the one suggested by Friedlander and Kennedy,[67] the Z_A formula obtained by considering maximum binding energy. The data fitted a normalized smooth curve very well with $\nu = 5$ and $\nu_H / \nu_L = 3 / 1$, still having one neutron boiled off before fission took place (see Fig. 16). (Incidentally, this is the curve that we used for all our chain-position and independent-yield calculations. Actually the smoothness of the yield-mass curve of U^{235} plus 45.7-Mev helium ions, obtained in this work after the independent-yields corrections using this curve, indicated that this

---

* We have also tried Levy's Z_A values, but these showed the same kind of discrepancy.

** Since, in using the ECD rule in our case, we have $Z_P = 47 \pm \frac{Z_{A_1} - Z_{A_2}}{2}$, where the plus sign is for the heavy fragment and the minus sign for the light fragment. A_1 refers to the heavy fragment and A_2 refers to its complementary fragment.

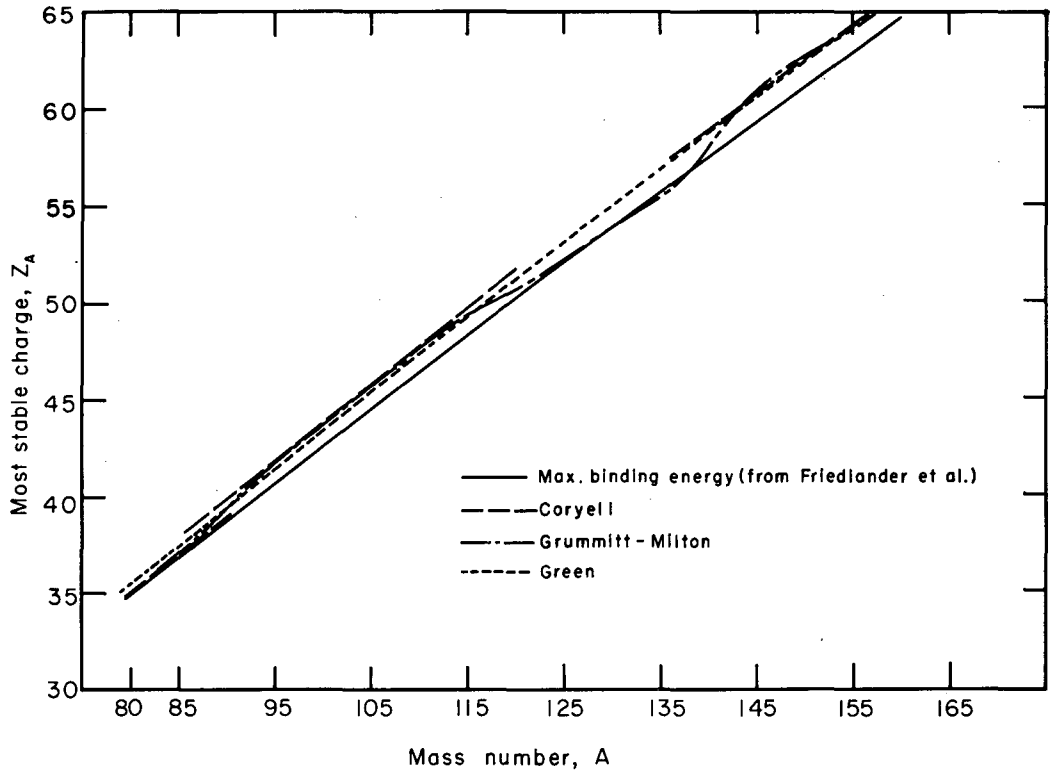

Fig. 15. Some of the commonly used distributions of most stable charge.

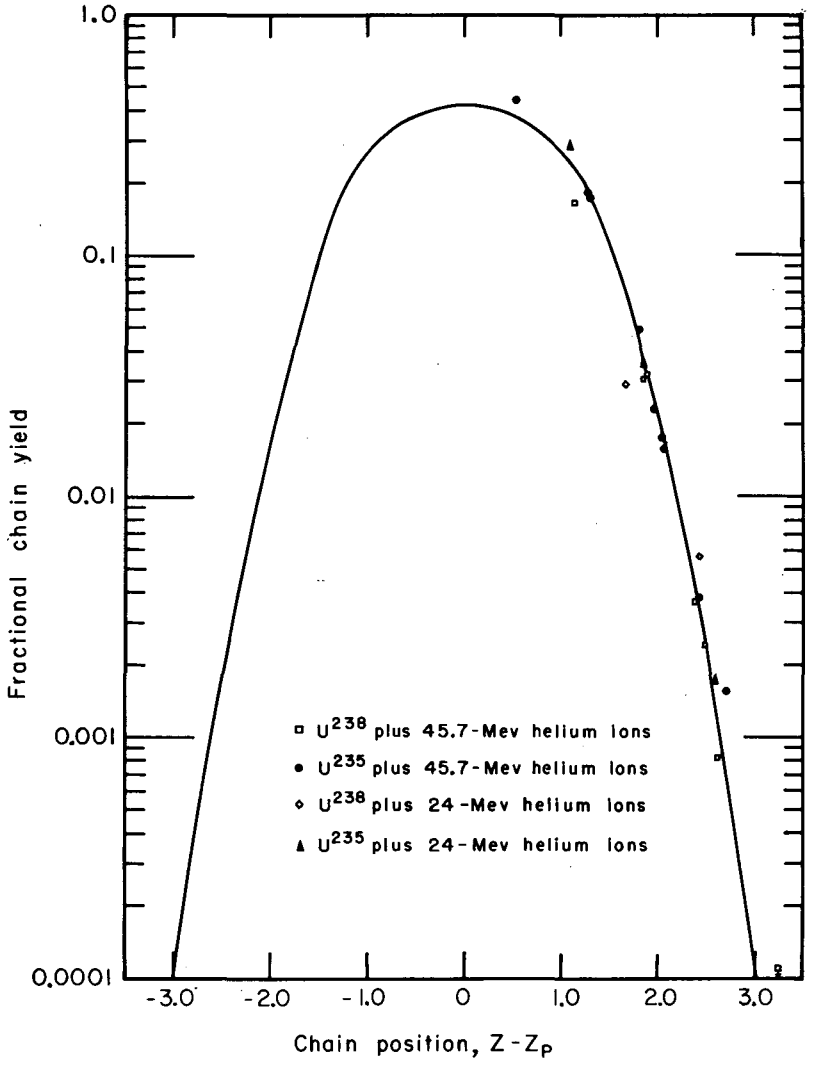

Fig. 16. Charge-distribution curve based on Z_A's of Friedlander and Kennedy.[67]

curve can be used as an empirical charge-distribution curve for similar bombardments like the one of Wahl for thermal-neutron fission of U^{235}.[56] The curve is also slightly different from a Gaussian curve. It has a broader half width and broader width on the wings than Wahl's curve). However, the empirical constants for this set of Z_A were taken from a rather old mass formula*, and is certainly not the best Z_A function available.

A better set of Z_A values from Green's treatment,[68] calculated according to the neutron-excess key function, was used.** The best fit was obtained by using $\nu = 5$ for the 45.7-Mev bombardments, and the equal division of the postfission neutrons between the two fragments. This plot is shown in Fig. 17. This fit definitely is not as good as the previous one. The general tendency to higher fractional chain yields of most of the cesium isotopes needs a larger neutron boil-off for the heavy fragments then for the light ones. The low yield for Cs^{136} from the fission of U^{238} by 24-Mev helium ions is obviously different from the behavior of the other cesium isotopes. Since it is always low among cesium isotopes in any kind of treatment, one might look for an explanation in the 82-neutron shell near by.†

The total number of emitted neutrons used in this work sounds quite low if one extrapolates Halpern's curve[63] to 40 Mev excitation energy (ν should be 7 instead of 5). One may argue that, in consideration of the different bombarding particle and the increasing neutron binding energy, it may be that the number of neutrons boiled off has leveled off somewhere above 20 Mev excitation energy. But this has almost been ruled out because the data for U^{235} at 20 Mev excitation energy give points about 0.4 charge unit below the data for U^{235} at 40

---

*This was pointed out by Dr. Swiatecki; in fact, the Z_A's fall well below the line of β stability traced out by the stable isotopes.

**This again is the kind suggestion of Dr. Swiatecki.

†All the Z_A's used and Z_p's calculated above are listed in Tables XIV and XV in the Appendix.

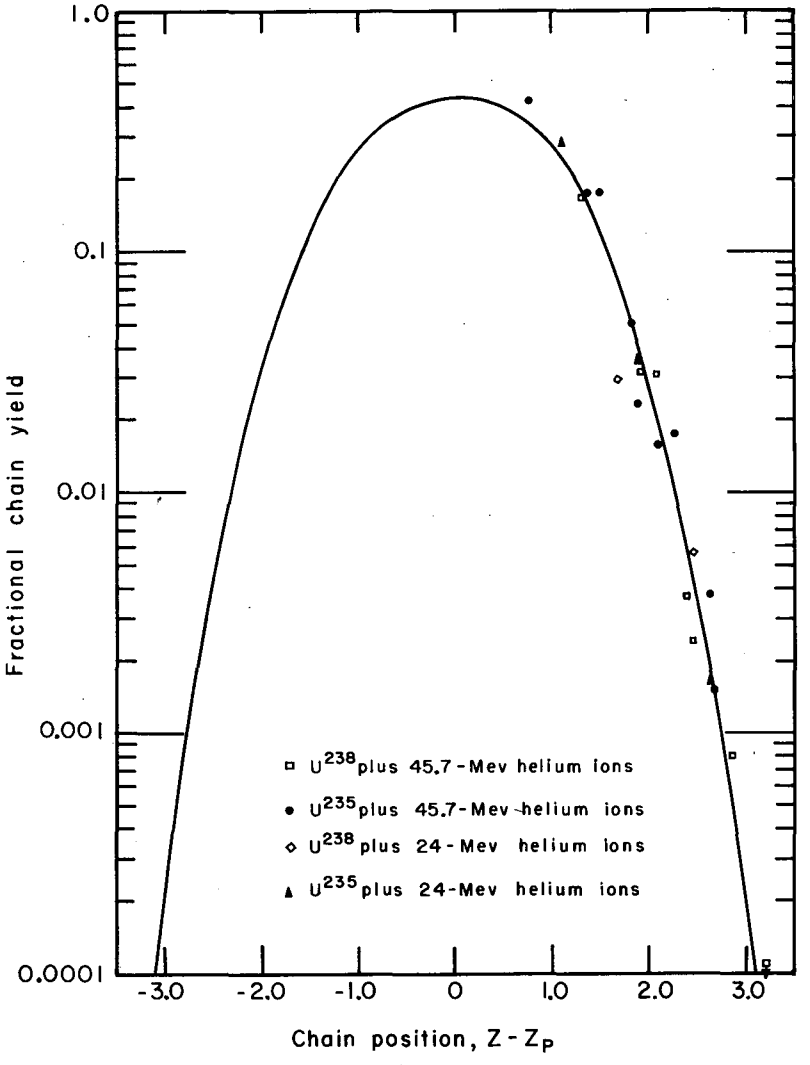

Fig. 17. Charge-distribution curve based on Green's Z_A values.[68]

Mev excitation energy on Fig. 9; and this means two fewer neutrons boiled off (i.e., 3 instead of 5). How does one reconcile this number with the experimentally measured number, 5 for U^{235} plus 14-Mev neutrons,[63] at roughly the same excitation energy? This would certainly require further experimental studies and any conclusive statement would be premature at present.

The best fit of the linear Z_A functions for the ECD rule implies that the shell effect does not enter into the fission process at this region of excitation. This is shown qualitatively in Fig. 9. Actually when the non-shell-affected Z_A is used, ECD has already lost its original meaning. Obviously the mechanism of thermal-neutron fission and that of the fission induced by charged particles at this excitation cannot be related by the "Equal-Charge-Displacment Rule" alone. The significance of the non-shell-effect in the fission studied in this work may mean that fission at this excitation is much faster than at lower excitation energy – the thermal neutron fission – and that the act of fission is not greatly affected by the shell properties of the fragments after fission takes place. (The word "greatly" is used here to reserve for the possibility that there is some residual shell effect that can explain the slight abnormality of the cesium isotopes, especially Cs^{136}. But up to this point, the author cannot propose any unique explanation for this). In this respect, it may seem inviting to consider the CCR rule for high-energy fission. In fact, the reasonable fit for the CCR rule did support the supposition that this may be applicable in part. The real difference between low-energy fission and high-energy fission apparently depends on something more than just the "ECD" and "CCR" rules, but rather on the details of the fission mechanisms themselves, and at this point is where the shell effect enters. The thermal-neutron fission of U^{235}, which is the typical example of low-energy fission, would still be best explained by this "shell-affected" ECD treatment; but the medium-excitation-energy fission (e.g., in this work, excitation at ~20 Mev or ~40 Mev) would be much closer to high-energy fission in general character. (The broader half width of the distribution curve does imply that there is a slight indication for superposition of fissioning nuclei; this agrees

with what Pate et al. observed,[58] and is discussed in the next section, on high-energy fission). Actually the real way to explain the fission at medium excitation energy may be an intermediate between the "non-shell-affected Z_A" ECD rule and the CCR rule. The matching of some of the cesium isotopes on the CCR curve that were off the ECD curve may indicate that this is the case. The conclusion reached by Gibson on the basis of his observations[24] certainly embodied the same idea.

The only comparable theoretical treatment in this respect would be that due to Present.[69] He used Wigner's model[70] and considered the electrostatic effect of the splitting, but did not take the nuclear shell structure into account. Swiatecki later simplified the whole treatment and gave a rather simple formula for calculating the charge-to-mass ratio of the fragments.[71] The calculated results from this simple formula gave the light fragments a higher charge-to-mass ratio than the heavy fragments. This certainly is in the right direction and does give the right order of magnitude. However, no detailed agreement can be expected, since the results of the calculations depend strongly on the effective distance between the two fragments at the point of fission (Present assumed the distance between the spherical fragments to be defined by the condition of tangency, but a more general treatment would keep the distance between the fragments as a parameter). Yet the general tendency does show that it would be worthwhile to continue along Present's approach and with Swiatecki's formulation. Further theoretical work would be necessary to help to interpret the experimental data.

The Independent Yields for High-Energy Bombardments

For 730-Mev Proton Bombardment.

The breadth and the asymmetric shape of the distribution of independent yields for cesium isotopes are the striking features. Both Hicks and Gilbert[72] and Pate et al.[58] have observed that as the energy of the bombarding particle increased, the charge distribution broadened. Pavlotskala and Lavrukhina have measured the fission yields of rare earth elements from uranium bombarded with 660-Mev protons;[39] however, their

measured data are not all independent yields, further, they used more interpolated points than measured points, making the comparison rather difficult. They didn't mention the broadening toward the higher-mass side and the asymmetric shape of the distribution.

In general, for high-energy reactions, a broad spectrum of excitation was assumed to be produced with corresponding complexity of the reaction products observed. And it would presumably be the multiplicity of fissioning nuclei and their various contributions to the yield of a given fission product that make the distribution as wide as it is.

This broad and asymmetric distribution toward the heavy-mass side does show that our results agree with what Lindner and Osborne observed:[33] at 340 Mev proton energy, they measured the spallation cross section and observed the presence of isotopes of uranium and protactinium of mass 237 to mass 227 in measurable yield. Since the cross section drops as more neutrons are boiled off, and the fissionability (Z^2/A) increases as the mass goes down (for the same Z), this certainty would result in a rather broad distribution, with the asymmetry toward the higher-mass side, and the "deep" emissive fission mechanism seems to be quite likely.[37]

Lindner and Osborne observed that the symmetry of the yield mass distribution might change at high energies.[29] Recently Stevenson et al. suggested that above 50 Mev bombarding energy, the yield mass distribution was not symmetrical about a given mass number at a given bombarding energy.[38] They observed that the heavy fragments had too low yields. We first thought the asymmetric-shaped independent yield distribution might be a contributing factor. From the above measured Cs fraction, we can see that the apparent peak lies on the neutron-deficient side--and this is more so for the rare earth elements (Eu^{157} was the heaviest isotope studied by Stevenson et al.), assuming a constant charge-to-mass ratio at the peak yield--whereas for the light fragments, the peak has shifted over to the neutron-excess side. The Rb fraction in this experiment gives a pretty good indication that this is the case. We have measured the independent yields of Rb^{84} and Rb^{86}, and have

estimated the independent yield of Rb^{83}. If the cesium data are used as an analog, this gives the apparent peak of the Rb fraction at mass 88.5, which places Rb^{86} corresponding to Cs^{129} (since the apparent peak for the Cs fraction was found to be at mass 131.5). Though there were no points on the neutron-excess side measured in the Rb fraction, the similarity between the two of the slope on the neutron-deficient side indicates that the independent yield distribution for the light fragments may not be widely different from that of the heavy fragments. From this we can say that Stevenson et al.[38] have measured nearly the total chain yields for the light fragments (Y^{90}, Y^{91}, and Y^{93}); but only partial chains for the heavy fragments, because of the widening of the independent-yield distribution toward the neutron-excess side. We have estimated the contributions of the yields beyond Eu^{156} and Eu^{157}, and they are only 12% and 15% of the total mass chain yield respectively. (We used the cesium independent-yield distribution, and the yield mass distribution obtained in this work.) Therefore the asymmetry of the independent yield distribution affects the yield mass distribution only slightly, certainly not by the large amount that they have observed.[38]

For the 100-Mev Carbon-Ion Bombardment.

The bombardment of U^{238} with 100-Mev carbon-ions gives independent yields of the Cs fraction which also features the broadened and asymmetric-shaped distribution. This certainly is not as striking as that of the 730-Mev proton-induced fission, but it still shares some of the features of the high-energy fission. Alexander observed* that the distribution of independent yields among iodine isotopes for the fission of U^{238} induced by 120-Mev carbon-ions did show the same effect.[73] But Blann, in his Au plus 120-Mev carbon-ion fission, observed* a narrower and more symmetric distribution in the iodine fraction.[74] The broadened and asymmetric-shaped distribution again can be explained by the multiplicity of fissioning nuclei and their various contributions to the yields of different isotopes. However, the Au fission is almost certainly different from the U fission with heavy ions in this respect.

*Radiochemical data.

The Mass Distribution

The smoothness of the yield mass curves for U^{238} bombarded with 45.7- and 24-Mev helium ions and U^{235} with 45.7-Mev helium ions apparently shows that there are no obvious perturbations (e.g. even-odd effect or shell effect) in this region. The slight scattered yields for U^{238} with 24-Mev helium ions cannot be taken very seriously, since it was a rather poor mass-analysis run. The increase of slope from U^{238} to U^{235} with the same energy and from the high-energy U^{238} target to low-energy U^{238} target were both expected and understandable. The slight change of the slope of the U^{235} yield mass curve is probably due to the change of the fissioning nuclei (from Pu^{241} to Pu^{238}).[75] The lowering of the yield mass curve for U^{238} with 24-Mev helium ions would account for the slight increase in slope.

The slope for the thermal-neutron fission of U^{235} is much steeper than the above ones, as one would expect. It is very similar, though, to the results of Petruska et al.[14]

One would wonder, at this point, what is the contribution of the induced fission in the target material due to the presence of the secondary neutrons in the cyclotron. Cobble measured this and stated that the secondary-neutron fission yields were about 1% of those for 43-Mev helium ions.[76] Allen and Ferguson measured the fission cross sections of U^{238} for neutrons in the energy range 0.03 to 3.0 Mev, and they found the cross section is very low below 1.5 Mev (0.2 barn), and leveled off from 1.4 to 3.0 Mev at 0.4 to 0.5 barn.[77] From these two one can see that the neutron flux cannot be large. (It is assumed that the energy of the secondary neutron is about 1 to 2 Mev). For U^{235}, Allen and Ferguson measured the cross section in this region as somewhere around 1.3 barns,[77] which is slightly lower than the fission cross-section with 45-Mev helium ions.[22] Therefore the contribution of induced fission by secondary neutrons in the U^{235} target cannot be much greater than in the U^{238} target. As for the secondary-thermal-neutron fission of U^{235}, the high fractional chain yields from the U^{235} target indicates that the contribution cannot be significant. If it does play a significant part,

thermal-neutron fission would give very low fractional chain yields, all the other indications (e.g., the slope of the yield mass curve) show that this is not the case.

The yield mass curve for fission of U^{238} induced by 730-Mev protons (shown in Fig. 6) represents roughly the character of high-energy fission. Since several assumptions are involved in obtaining this yield mass curve, it cannot be taken as seriously as some of the other yield mass curves reported here. But it does point out that the slope of the yield mass curve for high-energy fission is similar to that for medium-energy fission (24- and 45.7-Mev helium ions here). This slope is also quite similar to the existing high-energy proton-fission data; e.g., for the 340-Mev proton fission of uranium mentioned by Stevenson et al.,[38] this slope falls between their measured slope and the reflected slope from the light wing.

Pavlotskala and Lavrukhina pointed out, in their high-energy fission work, that from their data the fission of heavy elements by high-energy particles would not seem to be a likely mechanism for explaining the natural abundance of the rare earth elements.[39] But from the composition of the stable isotopes of Ce, Nd, and Sm obtained in this work after proper corrections for natural contamination, (shown in Table XIII along with the natural abundances of these elements), we found the general trend is somewhat similar to the natural abundances, after complete decay. Therefore, it is not impossible that some part of the formation of these elements (in the abundance in which they occur naturally) can be explained by the fission of heavy elements by high-energy particles. This alternative method of production may prove helpful in explaining the occurrence in high yield of extremely neutron-deficient stable isotopes such as Sm^{144}.

Table XIII

Compositions of stable isotopes of Ce, Nd, and Sm made in the fission of U^{238} induced by 730-Mev protons (compared with the natural compositions)

	Compositions (in percent)					
	Ce fraction		Nd fraction		Sm fraction	
Mass A	Natural	This work	Natural	This work	Natural	This work
136	0.193	6.4±0.1				
138	0.250	9.4±0.2				
140	88.48	56.2±2.3				
142	11.07	28.0±1.1	27.13	13.2±1.7[a]		
143			12.20	28.7±2.8		
144			23.87	14.4±2.2	3.16	3.6±0.3
145			8.29	16.9±2.6		
146			17.18	14.7±2.2		
147					15.07	38.2±2.7
148			5.72	7.8±1.2	11.27	9.1±0.7
149					13.82	27.3±1.8
150			5.60	4.3±0.6	7.47	5.5±0.5
152					26.63	10.9±0.9
154					22.53	5.5±0.4

[a] Sm^{146} has been added to Nd^{142} because of its α decay.

ACKNOWLEDGMENTS

I want to extend my grateful acknowledgment to Dr. Maynard C. Michel, under whose continual guidance and assistance this work was successfully completed. I also want to thank Professor David H. Templeton for his constant interest and encouragement during the course of these experiments.

The helpful suggestions and enlightening discussions of Dr. J. M. Alexander and Dr. W. J. Swiatecki are gratefully acknowledged. The kindness of Dr. Swiatecki and Dr. Alexander and Mr. Blann for allowing me to quote their unpublished results is greatly appreciated.

I want to thank Mr. Frederick L. Reynolds for helpful suggestions and assistance. Special thanks are due Messrs. George W. Kilian, Milton N. Firth, and Marion Davis for their excellent technical assistance during the course of this work.

I am much obliged to Mr. Bart Jones, Mr. Pete McWalters, and the crew of the 60-inch cyclotron; to Mr. James T. Vale and the crew of the 184-inch cyclotron and to Dr. Edward L. Hubbard and the crew of the Hilac for their excellent cooperation in performing the bombardments.

The help of the Health Chemistry Group is also very much appreciated.

I am grateful to Mrs. Lilly Y. Hirota for typing the Multilith originals for this thesis.

I wish to thank the China Institute in America for providing me a scientific fellowship during the first two years of this work.

This work was performed under the auspices of the United States Atomic Energy Commission.

APPENDIX

Table XIV

Mass A	Values for most stable charge Z_A Coryell[a]	Grummitt-Milton[b]	Friedlander[c]	Green[d]
84	36.59	36.65	36.44	37.03
85	36.97	36.95	36.83	37.43
86	37.36-38.20	37.35	37.22	37.83
87	37.74-38.60	37.85	37.61	38.23
88	38.13-38.99	38.40	38.00	38.63
89	38.51-39.39	38.83	38.40	39.04
98	42.96	42.95	41.89	42.62
99	43.36	43.35	42.28	43.01
100	43.76	43.75	42.66	43.40
101	44.16	44.16	43.04	43.79
102	44.55	44.57	43.43	44.19
103	44.95	45.00	43.81	44.58
104	45.35	45.25	44.20	44.97
105	45.74	45.65	44.57	45.36
106	46.14	46.05	44.96	45.75
131	54.25	54.10	54.29	55.34
132	54.60	54.46	54.65	55.71
133	54.95	54.70	55.02	56.09
134	55.30	55.02	55.39	56.46
135	55.65	55.35	55.75	56.84
136	56.00-57.40	55.70	56.12	57.21
137	56.35-57.76	56.25	56.48	57.59
138	56.70-58.11	56.90	56.85	57.96
139	57.05-58.47	57.40	57.21	58.33
140	57.40-58.83	58.02	57.57	58.71
148	61.68	62.10	60.45	61.67
149	62.04	62.40	60.80	62.04
150	62.40	62.70	61.16	62.40
151	62.76	62.90	61.52	62.77
152	63.11	63.15	61.87	63.14
153	63.47	63.50	62.23	63.51
154	63.83	63.70	62.58	63.87
155	64.18	64.10	62.94	64.24
156	64.54-64.00	64.43	63.30	64.60
157	64.37	64.70	63.65	64.97

[a] C. D. Coryell, Ann. Rev. Nuclear Sci. 2, 305 (1953).

[b] W. E. Grummitt and G. M. Milton, A Re-Assessment of Two Postulates of Charge Distribution in Fission In the Light of New Nuclear Data. CRC-694, Chalk River, Ontario, May 1957.

[c] G. Friedlander and J. W. Kennedy, Nuclear and Radiochemistry (John Wiley and Sons, Inc., N. Y. (1955) p. 50.

[d] A. E. S. Green, Phys. Rev. 95, 1006 (1954).

Table XV

Fractional chain yields and Z_p values for shielded nuclides

Target material	Helium-ion energy (Mev)	Shielded nuclides	Fractional chain yields	Z_p*				
				ECD				
				Pappas	G.and M.	Friedlander	Green	CCR
U^{238}	45.7	Rb^{84}	0.00011	33.01-33.59	33.62	33.77	33.79	33.54
		Rb^{86}	0.00243±0.00005	34.33-34.76	34.45	34.51	34.56	34.32
		Cs^{131}	0.000097±0.000007	51.01	50.95	52.03	51.78	51.88
		Cs^{132}	0.00081±0.00002	51.38	51.24	52.40	52.16	52.27
		Cs^{134}	0.0309±0.0002	52.13-52.83	52.03	53.14	52.93	53.05
		Cs^{136}	0.1671±0.0040	52.88-53.58	52.95	53.89	53.69	53.83
		Pm^{150}	0.0318±0.0009	58.86-59.30	59.16	59.11	59.05	59.29
		Eu^{154}	0.00374±0.0002	59.84-60.26	60.74	60.61	60.59	60.85
	24	Cs^{134}	0.00575±0.00040	51.76	51.65	52.58	52.55	52.66
		Cs^{136}	0.0292±0.0020	52.50-53.21	52.50	53.33	53.31	53.44
U^{235}	45.7	Rb^{84}	0.00157±0.00004	34.13-34.54	34.10	34.30	34.34	33.97
		Rb^{86}	0.0231±0.0008	34.86-35.30	34.85	35.05	35.11	34.76

Table XV (cont'd.)

Target material	Helium-ion energy (Mev)	Shielded nuclides	Fractional chain yields	Z_P*				
					ECD			
				Pappas	G.and M.	Friedlander	Green	CCR
		Cs^{131}	0.0038±0.0001	51.60	51.53	52.60	52.37	52.53
		Cs^{132}	0.0175±0.0006	51.98	51.89	52.97	52.75	52.92
		Cs^{134}	0.1834±0.0023	52.72-53.42	52.57	53.72	53.51	53.71
		Cs^{136}	0.4435±0.0085	53.47-54.18	53.58	54.46	54.24	54.50
		Pm^{148}	0.0158±0.0007	58.70-59.14	59.15	58.95	58.89	59.24
		Pm^{150}	0.1733±0.0110	59.46-59.88	59.90	59.70	59.66	60.03
		Eu^{154}	0.0496±0.0024	61.09-61.36	61.30	61.20	61.20	61.61
	24	Cs^{132}	0.00167±0.00009	51.60	51.53	52.41	52.37	52.53
		Cs^{134}	0.0359±0.0006	52.35	52.18	53.16	53.13	53.32
		Cs^{136}	0.2847±0.0060	53.10-53.80	53.05	53.91	53.90	54.11

*$\nu = 5$ was used for 45.7-Mev bombardments and $\nu = 3$ used for 24-Mev bombardments; $\nu_H/\nu_L = 1$ for all cases except the column under Friedlander, where $\nu_H/\nu_L = 3/1$ was used.

List of Illustrations

List of Illustrations (cont'd.)

List of Tables

REFERENCES

1. M. G. Inghram, Ann. Rev. Nuclear Sci. 4, 81 (1954); J. Phys. Chem. 57, 809 (1953).
2. H. G. Thode, Nucleonics (No. 3) 3, 14 (1948).
3. H. G. Thode and R. L. Graham, Can. J. Res. A, 25, 1 (1947).
4. J. Macnarama, C. B. Collins, and H. G. Thode, Phys. Rev. 78, 129 (1950).
5. M. G. Inghram, R. J. Hayden, and D. C. Hess, Phys. Rev. 79, 271 (1950).
6. Glendenin, Steinberg, Inghram, and Hess, Phys. Rev. 84, 860 (1951).
7. Wiles, Smith, Horsley, and Thode, Can. J. Phys. 31, 419 (1953).
8. R. K. Wanless and H. G. Thode, Can. J. Phys. 33, 541 (1955).
9. Melaika, Parker, Petruska, and Tomlinson, Can. J. Chem. 33, 830 (1955).
10. T. J. Kennett and H. G. Thode, Phys. Rev. 103, 323 (1956).
11. Steinberg, Glendenin, Inghram, and Hess, Phys. Rev. 95, 867 (1954).
12. W. H. Fleming, R. H. Tomlinson, and H. G. Thode, Can. J. Phys. 32, 522 (1954).
13. J. A. Petruska, E. A. Melaika, and R. H. Tomlinson, Can. J. Phys. 33, 640 (1955).
14. J. A. Petruska, H. G. Thode, and R. H. Tomlinson, Can. J. Phys. 33, 693 (1955).
15. L. E. Glendenin et al., quoted by E. P. Steinberg and L. E. Glendenin in Proceedings of the International Conference on the Peaceful Uses of Atomic Energy, Geneva, (United Nations, N. Y., 1956) 7, 3.
16. A. T. Blades, W. H. Fleming, and H. G. Thode, Can. J. Chem. 34, 233 (1956).
17. Kukavadze, Anikina, Goldin, and Ershler, Conference of the Academy of Sciences of the USSR on the Peaceful Uses of Atomic Energy, July 1-5, 1955, English translation: AEC-Tr-2435 (1956), p. 125.
18. Ivanov, Gorshkov, Anikina, Kukavadze, and Ershler, The Soviet J. of Atomic Energy 3, 1436 (1957).
19. V. K. Gorshkov, R. N. Ivanov, G. M. Kukavadze, and I. R. Reformatsky, The Soviet J. of Atomic Energy 3, 729 (1957).
20. Susanne E. Ritsema, Fission and Spallation Excitation Functions of U^{238} (M. S. Thesis), UCRL-3266, Jan. 1956.

21. Wade, Gonzalez-Vidal, Glass, and Seaborg, Phys. Rev. 107, 1311 (1957).
22. Vandenbosch, Thomas, Vandenbosch, Glass, and Seaborg, Spallation-Fission Competition in Heaviest Elements; Helium Ion-Induced Reactions in Uranium Isotopes, UCRL-8032, Nov. 1957.
23. T. Darrah Thomas, Spallation-Fission Competition from the Compound System U^{233} plus He^{4}. (Thesis), UCRL-3791, July 1957.
24. Walter M. Gibson, Fission and Spallation Competition from the Intermediate Nuclei Americium-241 and Neptunium-235 (Thesis), UCRL-3493, Nov. 1956.
25. Richard M. Lessler, Spallation-Fission Competition in Neptunium Compound Systems. Decay-Scheme Studies (Thesis), UCRL-8439, Oct. 1958.
26. P. R. O'Connor and G. T. Seaborg, Phys. Rev. 74, 1189 (1948).
27. J. Jungerman, Phys. Rev. 79, 632 (1950).
28. E. M. Douthett and D. H. Templeton, Phys. Rev. 94, 128 (1954).
29. M. Lindner and R. N. Osborne, Phys. Rev. 94, 1323 (1954).
30. R. L. Folger, D. C. Stevenson, and G. T. Seaborg, Phys. Rev. 98, 107 (1955).
31. Vinogradov, Alimarin, Baranov, Lavrukhina, Baranova, Pavlotskaya, Bragina, and Yakovlev, in Conference of the Academy of Sciences of the USSR on the Peaceful Uses of Atomic Energy, July 1-5, 1955, AEC-Tr-2435,(1956) p. 65.
32. Hicks, Stevenson, Gilbert, and Hutchin, Phys. Rev. 100, 1284 (1955).
33. M. Lindner and R. N. Osborne, Phys. Rev. 103, 378 (1956).
34. N. S. Ivanov and I. I. P'ianor, Soviet Physics JETP 4, 367 (1957).
35. Aagaard, Andersson, Bergman, and Pappas, J. Inorg. Nuclear Chem. 5, 105 (1957).
36. A. K. Lavrukhina and L. D. Krasavina, J. Nucl. Energy 5, 236 (1957).
37. V. P. Shamov, Soviet Physics JETP 6, 268 (1958).
38. Stevenson, Hicks, Nervik, and Nethaway, Phys. Rev. 111, 886 (1958).
39. F. I. Pavlotskala and A. K. Lavrukhina, Soviet Physics JETP 7, 732 (1958).
40. L. E. Glendenin, C. D. Coryell and R. R. Edwards, in The National Nuclear Energy Series, Div. IV, (McGraw-Hill Book Co., N.Y., 1951) Vol. 9, Paper 52.

41. Alexis C. Pappas, A Radiochemical Study of Fission Yields in the Region of Shell Perturbations and the Effect of Closed Shells in Fission, AECU-2806, Sept. 1953.

42. A. C. Pappas, in Proceedings of the International Conference on the Peaceful Uses of Atomic Energy, Geneva, 1955 (United Nations, N. Y., 1956), 7, 19.

43. W. E. Grummitt and G. W. Milton, J. Inorg. Nuclear Chem. 5, 93 (1957). W. E. Grummitt and G. W. Milton, A Re-Assessment of Two Postulates of Charge Distribution in Fission in the Light of New Nuclear Data, CRC-694, Chalk River, Ontario, May 1957.

44. E. P. Steinberg and L. E. Glendenin, Proceedings of the International Conference on the Peaceful Uses of Atomic Energy, Geneva, 1955 (United Nations, N. Y., 1956), 7, 3.

45. R. H. Goeckerman and I. Perlman, Phys. Rev. 76, 628 (1949).

46. J. M. Alexander and C. D. Coryell, Phys. Rev. 108, 1274 (1957).

47. Patrick del Marmol, Medium Energy Deuteron and Alpha Fission of U^{235} (Thesis), Massachusetts Institute of Technology, Jan. 1959.

48. W. A. Aron, B. G. Hoffman, and F. C. Williams, Range-Energy Curves, AECU-663, May 1951.

49. Rosemary J. Barrett, Range-Energy Curves for Carbon Ion, Lawrence Radiation Laboratory, Berkeley, California, unpublished data.

50. W. E. Nervik, J. Phys. Chem. 59, 690 (1955).

51. K. A. Kraus and F. Nelson, in Proceedings of the International Conference on the Peaceful Uses of Atomic Energy, Geneva, 1955 (United Nations, N. Y., 1956), 7, 113.

52. H. Palevsky, R. K. Swank, and E. Gvenchik, Rev. Sci. Instr. 18, 298 (1947).

53. A. O. Nier, Rev. Sci. Instr. 18, 398 (1947).

54. C. M. Stevens, Rev. Sci. Instr. 24, 148 (1953).

55. D. Strominger, J. M. Hollander, and G. T. Seaborg, Revs. Modern Phys. 30, 585 (1958).

56. A. C. Wahl, J. Inorg. Nuclear Chem. 6, 263 (1958).

57. C. D. Coryell, Massachusetts Institute of Technology, private communication to J. M. Alexander, Lawrence Radiation Laboratory, Berkeley, California.

58. B. D. Pate, J. S. Foster, and L. Yaffe, Can. J. Chem. 36, 1705 (1958).

59. R. L. Ferguson, Nuclear Charge Distribution Curves in Fission: Independent Yields of Sr^{91}, Ba^{139} and Ba^{140} from Thermal-Neutron Fission of U^{235} (Thesis), Washington University, 1959.

60. David E. Troutner, Nuclear Charge Distribution in Fission: Independent Yields of Niobium Isotopes from Thermal-Neutron Fission of U^{233}, U^{235} and Pu^{239} (Thesis), Washington University, Aug. 1959.

61. E. K. Hyde and G. T. Seaborg, The Transuranium Elements in Handbuch der Physik, Vol. 42 (Springer Verlag, 1957).

62. B. M. Foreman, Jr., Spallation and Fission Competition in Thorium-232 and the Masses of the Heaviest Elements, (Thesis), UCRL-8223, April 1958.

63. I. Halpern, "Nuclear Fission", University of Washington (1959). (Prepared for the Annual Reviews of Nuclear Science).

64. C. D. Coryell, Ann. Rev. Nuclear Sci. 2, 305 (1953).

65. A. G. W. Cameron, A Revised Semi-Empirical Atomic Mass Formula, CRP-690, Chalk River, Ontario, March 1957.

66. H. B. Levy, Phys. Rev. 106, 1265 (1957).

67. G. Friedlander and J. W. Kennedy, Nuclear and Radiochemistry (John Wiley and Sons, Inc., N. Y., 1955) p. 50.

68. A. E. S. Green, Phys. Rev. 95, 1006 (1954).

69. R. D. Present, Phys. Rev. 72, 7 (1947).

70. E. Wigner, University of Pennsylvania Bicentennial Conference (1941).

71. Wladyslaw J. Swiatecki, Proc. Phys. Soc. (London) A, 63, 1208 (1950); Wladyslaw J. Swiatecki, UCRL, private communication.

72. H. G. Hicks and R. S. Gilbert, Phys. Rev. 100, 1286 (1955).

73. John M. Alexander, UCRL, private communication.

74. H. Marshall Blann, UCRL, private communication.

75. Ellis P. Steinberg, ANL, private communication.

76. James W. Cobble, The Chemistry and Nuclear Chemistry of the Heavy Elements, Progress Report No. 3, AECU-3663, 1958.

77. W. D. Allen and A. T. G. Ferguson, Proc. Phys. Soc. (London) A, 70, 573 (1957).